

CrossMark
click for updates

Cite this: DOI: 10.1039/c6cy00335d

Hydrogenation of dicarboxylic acids to diols over Re–Pd catalysts†

Yasuyuki Takeda,^a Masazumi Tamura,^a Yoshinao Nakagawa,^a Kazu Okumura^b
and Keiichi Tomishige^{*a}

A Re–Pd/SiO₂ (Re/Pd = 8) catalyst was applied to hydrogenation of dicarboxylic acids (succinic acid, glutaric acid and adipic acid) to diols. In the hydrogenation of dicarboxylic acids, *ex situ* liquid-phase (in only 1,4-dioxane solvent) reduced Re–Pd/SiO₂ showed much higher activity than *in situ* liquid-phase (in the mixture of dicarboxylic acid and 1,4-dioxane) and gas-phase reduced ones, in which the *in situ* liquid-phase reduced catalyst has been reported to show good activity in the hydrogenation of monocarboxylic acids. High diol yields (71–89%) were achieved in the hydrogenation of dicarboxylic acids on the *ex situ* liquid-phase reduced catalyst at 413 K. Lactones and hydroxycarboxylic acids were first formed as intermediates in the reaction of C4–C5 and ≥C6 dicarboxylic acids, respectively. Characterization using XRD, XPS and XAS indicates that *ex situ* liquid-phase reduced catalysts with high activity contains comparable amounts of Re⁰ and Reⁿ⁺ species, both of which have been reported to be necessary for good performance. The amount of Reⁿ⁺ species on the *in situ* liquid-phase reduced catalysts is much larger than that of surface Re⁰ species. This result suggests that the presence of dicarboxylic acids suppresses the reduction of Re species to Re⁰ on the calcined catalysts while that of monocarboxylic acids does not, which leads to the low activity in the hydrogenation of dicarboxylic acids on *in situ* liquid-phase reduced catalysts.

Received 12th February 2016,
Accepted 6th April 2016

DOI: 10.1039/c6cy00335d

www.rsc.org/catalysis

Introduction

Biomass is an abundant and environmentally friendly resource in place of petroleum because biomass is the only renewable resource with organic carbons, and the conversion of biomass to valuable chemicals is an important and urgent research topic.¹ Among various biomass-derived chemicals, succinic acid (SUC) has recently attracted much attention as a promising platform chemical² because SUC can be easily produced by the fermentation of sugar (potential production of SUC: 64 000 tons per year (in 2015)³) and the production cost of the fermentation method is estimated to be much lower than that of the conventional method of SUC production from petroleum.⁴ Various transformation methods of SUC have been developed, which can produce valuable chemicals such as 1,4-butanediol (1,4-BuD), *N*-methyl-2-pyrrolidone, 2-pyrrolidone, succinimide, succinic esters and maleic acid.⁵ Among these methods, hydrogenation of SUC to 1,4-BuD is one of the important

reactions^{1c,5,6} because 1,4-BuD is an important raw material for thermoplastic polymers such as polybutylene succinate (PBS) and polybutylene terephthalate (PBT).^{1h} However, 1,4-BuD is conventionally produced by the transformation of petroleum such as the catalytic hydrogenation of maleic anhydride,⁷ and biomass-derived 1,4-BuD has been required for the production of biopolymers.⁸ In addition, other dicarboxylic acids such as adipic acid (ADI) and glutaric acid (GLU) can be produced in the oxidation of a mixture of cyclohexanol and cyclohexanone derived from petroleum,⁹ and hydrogenation of these dicarboxylic acids can also give diols which are important materials for the production of polymers.^{8b} Therefore, effective catalysts for the hydrogenation of biomass- and petroleum-derived dicarboxylic acids to diols are desired to be developed.

Effective homogeneous catalysts such as H₄Ru₄(CO)₈(PBU₃)₄ (ref. 6*m*) and heterogeneous catalysts such as Re₂O₇, Ru–Sn-based catalysts, M/C (M = Pd, Pt, Rh) and Re species + noble metal catalysts^{6a–l} for the hydrogenation of dicarboxylic acids to diols have been reported. From the viewpoint of the recovery and reusability of the catalysts, heterogeneous catalysts are more preferable than homogeneous ones.^{6l} In the hydrogenation of SUC, the Re catalyst obtained by *in situ* reduction of Re₂O₇ has been known to be effective for the reaction for a long time, providing 94% yield of 1,4-BuD (483 K, 25 MPa H₂, no solvent).^{6a} In the case of supported catalysts, Re species + noble metal catalysts

^a Department of Applied Chemistry, School of Engineering, Tohoku University, 6-6-07 Aoba, Aramaki, Aoba-ku, Sendai 980-8579, Japan.

E-mail: tomi@erec.che.tohoku.ac.jp

^b Department of Applied Chemistry, Faculty of Engineering, Kogakuin University, 1-24-2 Nishi-Shinjuku, Shinjuku-ku, Tokyo 163-8677, Japan

† Electronic supplementary information (ESI) available. See DOI: 10.1039/c6cy00335d

provided high yields of 1,4-BuD (Re(3.6 wt%)-Pd(2 wt%)/TiO₂: 83% (solvent: H₂O),^{6h} Pd(1 wt%)-Re(4 wt%)/TiO₂: 86% (solvent: 1,4-dioxane and H₂O),^{6j} Re(0.3 mol%)-Ru(0.3 mol%)/mesoporous carbon (MC): 71% (solvent: 1,4-dioxane)^{6k}) under the conditions of $T = 433\text{--}473\text{ K}$ and $P_{\text{H}_2} = 6.9\text{--}25\text{ MPa}$. In the hydrogenation of mixtures of SUC, GLU and ADI, the Ru(5 wt%)-Sn(3 wt%)-Re(5 wt%)/C catalyst (453 K, 15 MPa H₂, solvent: H₂O) provided high yields of 1,4-BuD (75%), 1,5-pentanediol (98%) and 1,6-hexanediol (96%), respectively.^{6l} In addition, Re species + noble metal catalysts have been reported to be also active in the hydrogenation of maleic acid¹⁰ and monocarboxylic acids^{11–13} to alcohols. Therefore, catalysts including Re species are efficient for the hydrogenation of dicarboxylic acids to diols.

In our previous work, we also reported that the Re-Pd/SiO₂ catalyst with a high Re loading amount (Re = 14 wt%, Pd = 1 wt%, Re/Pd = 8) showed high selectivity and yield of 1-octadecanol (94%) in the hydrogenation of stearic acid (STA) under comparatively mild conditions ($T = 413\text{ K}$, $P_{\text{H}_2} = 8\text{ MPa}$, solvent: 1,4-dioxane).^{11,12} Characterization of the Re-Pd/SiO₂ catalyst suggests the effective structure of the Re⁰ surface modified with Re^{*n*+} ($n = 3$ or 4) species, which was responsible for the high activity. In addition, the catalyst activity was greatly influenced by the reduction method of the catalyst; liquid-phase reduction in the reaction mixture (*in situ* reduction method) showed much higher activity for the reaction than *ex situ* gas-phase reduction. A similar tendency was also observed in the case of Re₂O₇,^{6a} where *in situ* reduction of Re₂O₇ provided a higher 1,4-BuD yield (94%) than *ex situ* reduction (35%) in the hydrogenation of SUC. These results indicate that the structure of Re-based catalysts is largely influenced by the reduction method of the catalysts, and the selection of an appropriate reduction method is essential to obtain high performance of the catalysts in the objective reaction.

Herein, we applied the Re-Pd/SiO₂ (Re = 14 wt%, Pd = 1 wt%, Re/Pd = 8) catalyst to the hydrogenation of dicarboxylic acids to diols, and we found that the catalyst was also effective for the reaction. The catalyst system was applicable to the hydrogenation of various dicarboxylic acids to afford the corresponding diols in high yields (71–89%). In this catalyst system, the selection of the reduction method was very important to obtain high activity of the catalyst, and the *ex situ* liquid-phase reduction method, where the catalyst was reduced in only 1,4-dioxane solvent without any substrates, showed higher activity in the hydrogenation of SUC than the other reduction methods. The catalyst was also characterized by means of X-ray diffraction (XRD), X-ray absorption spectroscopy (XAS) and X-ray photoelectron spectroscopy (XPS). The dependence of the catalytic activity on the reduction method was discussed on the basis of the catalyst structure.

Experimental

Catalyst preparation

M'/SiO₂ (M' = Pd, Ru, Rh, Ir and Pt, 1 wt%) and M''/SiO₂ (M'' = Re, Mo, W and Ti, 14 wt%) catalysts were prepared by im-

pregnating silica (G-6, BET surface area 535 m² g⁻¹, Fuji Silysia Chemical, Ltd.) with an aqueous solution of RuCl₃ (Kanto Chemical Co., Ltd.), RhCl₃ (Soekawa Chemical Co., Ltd.), PdCl₂ (Wako Pure Chemical Industries, Ltd.), H₂PtCl₆ (Kanto Chemical Co., Ltd.), H₂IrCl₆ (Furuya Metals Co., Ltd.), (NH₄)₆Mo₇O₂₄ (Wako Pure Chemical Industries, Ltd.), NH₄ReO₄ (Soekawa Chemical Co., Ltd.), (NH₄)₁₀W₁₂O₄₂ (Wako Pure Chemical Industries, Ltd.) and TiCl₃ aq. (20%, Wako Pure Chemical Industries, Ltd.). After impregnation, the obtained wet catalysts were dried at 383 K for 12 h, and then they were calcined in air at 673 K for 3 h. M''-M'/SiO₂ catalysts were prepared by impregnating M'/SiO₂ catalysts after drying at 383 K for 12 h. In the case of M''-Pd/SiO₂ catalysts, the loading amount of M'' is represented as the molar ratio of M'' to Pd (for example, M''/Pd = 8). On the other hand, in the case of Re-M'/SiO₂ catalysts (M' = Ru, Rh, Ir and Pt), the loading amount of M' is represented by the molar ratio of Re to M' (for example, Re/M' = 8). The Re loading amount of the Re-Pd/SiO₂ (Re/Pd = 8) catalyst is the same as that of the Re/SiO₂ (Re = 14 wt%) catalyst. The preparation method for Re-Pd/SiO₂ is the same as that in our previous work.¹¹ All catalysts were used in powdery form.

Activity tests

Activity tests were performed using a stainless steel autoclave (190 ml) with an inserted glass vessel. The catalyst was set in the glass vessel with a spinner, succinic acid (SUC, Wako Pure Chemical Industries, Ltd., >99.5%) and an appropriate amount of 1,4-dioxane (Wako Pure Chemical Industries, Ltd., >99.5%) as a solvent. The pretreatment of the catalyst was described below. The solvent was selected because of the solubility of the carboxylic acids used in this study. The substrates are listed in Table S1 in the ESI.† The glass vessel with the reagents was inserted into the autoclave, and after sealing the reactor, the air content in the autoclave was purged with 1 MPa H₂ (99.99%, Showa Denko K.K.) three times. The autoclave was heated to the desired temperature (typically, 413 K), and the H₂ pressure was increased to the appropriate pressure. The stirring rate was 500 rpm (magnetic stirring). After the reaction, the reactor was cooled down in a water bath, and the gas contents were collected in a gas bag. The liquid contents were transferred to a vial, and the catalyst was separated by centrifugation. The standard reaction conditions for the hydrogenation of SUC to 1,4-BuD are as follows: 1.0 g of SUC (8.5 mmol), 19 g of 1,4-dioxane, 100 mg of catalyst, 8.0 MPa hydrogen pressure (at 413 K), 413 K, 4 h. Reduction of the catalysts was conducted by three different methods: (1) *ex situ* liquid-phase reduction without SUC (*exL*), (2) *in situ* reduction with SUC (*inL*) and (3) gas-phase reduction (G). In method (1), the calcined catalysts were reduced in an autoclave with a spinner and 1,4-dioxane (19 g) without the substrate. After sealing the reactor, the reactor was purged with 1 MPa H₂ and then heated to 413 K. The autoclave was pressurized to 8 MPa H₂, and the content was stirred for 1 h. The catalysts are called “*ex situ* liquid-phase

reduced catalysts" and denoted, for example, as Re–Pd(*exL*, 413), where *exL* means "ex situ liquid-phase" and 413 means the reduction temperature. After cooling down to room temperature, the autoclave was opened and the substrate was added into the autoclave reactor in N₂ atmosphere, where all the procedures were carried out without exposure of the catalyst to air. The catalyst samples after the activity test are denoted as Re–Pd(*exL*, 413, Reaction) catalyst. In method (2), the calcined catalyst was *in situ* reduced during the heating step of the activity test by hydrogen in the presence of the substrate and the solvent. The catalysts are called "in situ liquid-phase reduced catalysts" and denoted, for example, as Re–Pd(*inL*, 413), where *inL* means "in situ liquid-phase". In addition, the samples after the activity test are denoted as Re–Pd(*inL*, 413, Reaction) catalyst. In method (3), the calcined catalysts were reduced in the gas phase under hydrogen flow. The calcined catalysts were reduced in H₂ flow (100% H₂, 30 mL min⁻¹) at 473 K for 1 h by using a gas flow system and a glass tube. The obtained catalysts are called "gas-phase reduced catalysts" and denoted, for example, as Re–Pd(*G*, 473), where *G* means gas-phase. The reduced catalyst and the substrate were introduced into an autoclave under N₂ atmosphere in order to avoid exposing the catalyst to air. The samples after the activity test are denoted as Re–Pd(*G*, 473, Reaction) catalyst.

The products were analyzed using gas chromatographs (Shimadzu GC-2025 and GC-2015) equipped with an FID. An HP-FFAP capillary column (diameter 0.25 mm, 30 m) was used for the separation of products in the liquid-phase such as γ -butyrolactone (GBL), 1,4-butanediol (1,4-BuD), tetrahydrofuran (THF), butyric acid (BA) and 1-butanol (BuOH). SUC was analyzed using a high performance liquid chromatograph (Shimadzu Prominence) equipped with a UV-vis detector and a refractive index detector. An Aminex HPX-87H column (Bio-Rad) was used for the separation. A Porapak N (diameter 3.0 mm, 3.0 m) packed column was used for the analysis of gaseous products such as CO₂, CH₄ and C₂H₆. The conversion, selectivity, averaged conversion rate (ν) [mmol g_{cat}⁻¹ h⁻¹] and quasi-formation rate of 1,4-BuD ($r_{1,4\text{-BuD}}$) [h⁻¹] are calculated on a carbon basis and defined in eqn (1)–(4):

$$\text{Conversion [\%]} = \frac{\sum(\text{product [mol]}n_{\text{product}}/n_{\text{substrate}})}{(\text{unreacted substrate[mol]}) + \sum(\text{product [mol]}n_{\text{product}}/n_{\text{substrate}})} \times 100 \quad (1)$$

$$\text{Selectivity [\%]} = \frac{(\text{product [mol]}n_{\text{product}}/n_{\text{substrate}})}{\sum(\text{product [mol]}n_{\text{product}}/n_{\text{substrate}})} \times 100 \quad (2)$$

$$\text{Averaged conversion rate } (\nu) [\text{mmol g}_{\text{cat}}^{-1} \text{h}^{-1}] = \frac{\sum(\text{product [mmol]}n_{\text{product}}/n_{\text{substrate}})}{(\text{reaction time [h]})(\text{the amount of catalyst [g]})} \quad (3)$$

$$\begin{aligned} \text{Quasi-formation rate } (r_{1,4\text{-BuD}}) [\text{h}^{-1}] \\ = \frac{\sum(\text{the product amount of 1,4-BuD [mmol]})}{(\text{reaction time [h]})(\text{the loading amount of metal [mmol]})} \end{aligned} \quad (4)$$

where $n_{\text{substrate}}$ and n_{product} are the carbon numbers in a substrate and a product, respectively. Products were also identified using GC-MS (QP-2010, Shimadzu). The mass balance was also confirmed for each result and the difference in mass balance was in the range of the experimental error ($\pm 5\%$), unless otherwise noted.

Catalyst characterization

Characterization of the catalysts was carried out in a manner similar to that of our previous report.¹¹ The detailed methods are described in the ESI.†

X-ray diffraction (XRD) patterns were recorded using a diffractometer (MiniFlex600, Rigaku). Cu K α ($\lambda = 0.154$ nm, 45 kV, 40 mA) radiation was used as the X-ray source. The catalyst samples after the reaction or reduction were transferred to an atmosphere separator (air-sensitive sample holder, Rigaku Corporation) using a glove bag under N₂ atmosphere to avoid exposing the samples to air. The particle size (d) on the catalysts was calculated by using Scherrer's equation.¹⁴ The XRD patterns were fitted by some Gaussian functions^{11,15} expressed.

XAS was carried out at the BL01B1 station of SPring-8 with the approval of the Japan Synchrotron Radiation Research Institute (JASRI; proposal no. 2014A1119, 2014B1248, 2015B1068). The storage ring was operated at 8 GeV, and a Si (111) single crystal was used to obtain a monochromatic X-ray beam. Ion chambers for I_0 were filled with 100% N₂ and 100% Ar for Re L₃-edge and Pd K-edge measurements, respectively. Ion chambers for I were filled with 50% N₂ + 50% Ar and 100% Kr for Re L₃-edge and Pd K-edge measurements, respectively. The samples after the reaction and reduction were prepared under the same conditions. After cooling, the prepared catalyst powder was transferred to a commercially

available polymer UV/Vis cell (UV-Cuvette micro 8.5 mm, BRAND GMBH + CO KG) in a glove bag filled with nitrogen to avoid exposure to air. The thickness of the cell filled with the powder was 2 mm to give an edge jump of 0.4–1.1 and 0.4–1.0 for Re L₃-edge and Pd K-edge measurement, respectively. The extended X-ray absorption fine structure (EXAFS) data for Re L₃-edge were collected in a transmission mode measurement, and those for Pd K-edge were collected in a fluorescence mode measurement. Analyses of EXAFS and X-ray absorption near edge spectral (XANES) data were

performed using a computer program (REX2000 ver. 2.6.0, Rigaku Corp.).

X-ray photoelectron spectroscopy (XPS) experiments were conducted with an AXIS-ULTRA DLD (Shimadzu Co., Ltd.) using monochromatic Al K α X-ray radiation ($h\nu = 1486.6$ eV) operated at 20 mA and 15 kV at room temperature under 10^{-8} Pa. The binding energy was calibrated with C 1s (284.6 eV). The catalysts after the reaction or reduction were transported to the analysis chamber in nitrogen atmosphere to avoid any exposure to air. Analysis of XPS data was performed by using the computer program CasaXPS ver. 2.3.15 (Casa Software, Ltd.). XPS patterns were fitted by the Voigt function.¹⁶ Re 4f_{7/2} and Re 4f_{5/2} are separated by 2.43 eV and have a relative peak area and a full width at half maximum (FWHM) with a fixed ratio of 4 : 3 and 1 : 1, respectively.¹⁷

Results and discussion

Catalytic performance of Re–Pd and related catalysts with different reduction methods in hydrogenation of succinic acid (SUC)

First, the effect of the reduction methods was investigated on the catalysts of Re–Pd/SiO₂ (Re = 14 wt%, Pd = 1 wt%, Re/Pd = 8) and Re/SiO₂ (Re = 14 wt%) in the hydrogenation of SUC (Table 1) because SUC is different from STA in terms of acidity and hydrophobicity. *In situ* liquid-phase reduction ((*inL*, *x*) series, the catalysts were reduced in SUC + 1,4-dioxane), gas-phase reduction ((*G*, *x*) series, the catalysts were reduced under hydrogen flow) and *ex situ* liquid-phase reduction ((*exL*, *x*) series, the catalysts were reduced in only 1,4-dioxane) were applied in this reaction. The detailed reduction methods are described in the experimental section. The Re–Pd(*exL*, 413) catalyst showed a higher averaged conversion rate (v) (5.4 mmol g_{cat}⁻¹ h⁻¹) than the Re–Pd(*inL*, 413) catalyst (0.8 mmol g_{cat}⁻¹ h⁻¹) and Re–Pd(*G*, 473) catalyst (2.2 mmol g_{cat}⁻¹ h⁻¹) (Table 1, entries 1–3) with high selectivity to GBL, which is an intermediate of the formation of 1,4-BuD as discussed below.^{1c,5,6h} On the other hand, THF, which can be produced from GBL,^{6k} was not observed in the case of all the catalysts, although GBL was observed. In addition, a similar tendency was also observed over the Re catalysts (Re-supported SiO₂) (Table 1, entries 4–6). As a result, the *ex situ* liquid-phase re-

duction is the most effective in the hydrogenation of SUC. In the case of hydrogenation of STA under similar reaction conditions (413 K, 8 MPa H₂),¹¹ the *in situ* liquid-phase reduced catalyst, Re–Pd(*inL*, 413), also showed an averaged conversion rate of 4.5 mmol g_{cat}⁻¹ h⁻¹ as high as that of the Re–Pd(*exL*, 413) catalyst (3.9 mmol g_{cat}⁻¹ h⁻¹), and the activity was similar to that (5.4 mmol g_{cat}⁻¹ h⁻¹) over the Re–Pd(*exL*, 413) catalyst in the hydrogenation of SUC. The difference in the suitable reduction method for the Re–Pd/SiO₂ catalyst between hydrogenation of STA and that of SUC can be derived from the difference in the substrate (SUC or STA), which implies that the presence of SUC suppresses the activation of the Re–Pd catalyst with H₂.

To confirm that Re–Pd/SiO₂ catalysts are truly effective for the hydrogenation of SUC, the reaction was performed using the *ex situ* liquid-phase reduced Re–M'/SiO₂ (M': Ru, Rh, Pd, Ir and Pt; Re = 14 wt%, Re/M' = 8) and M''–Pd/SiO₂ (M'': Re, Mo, W and Ti; Pd = 1 wt%, M''/Pd = 8) catalysts (Table 2). The monometallic Pd catalyst, Pd(*exL*, 413), showed no activity for the reaction (Table 2, entry 1). On the other hand, the monometallic Re catalyst, Re(*exL*, 413), showed moderate activity with high selectivity to GBL at 4 h (Table 2, entry 2). The addition of noble metals (Ru, Rh, Pd, Ir and Pt) to the Re catalyst enhanced the catalytic activity (Table 2, entries 3–7), and these catalysts also showed high selectivities to GBL ($\geq 88\%$) at 4 h. On the other hand, the Re–Pd(*exL*, 413) catalyst showed lower selectivities to hydrogenolysis products (BA and BuOH) than the other catalysts (Table 2, entries 3–7). In terms of the averaged conversion rate, Ir is a more effective noble metal than Pd (Table 2, entries 5 and 6). To assess the catalytic performance of the Re–Pd(*exL*, 413) and Re–Ir(*exL*, 413) catalysts, the activity test was conducted at longer reaction time (24–96 h) (Table 2, entries 8–11). The Re–Pd(*exL*, 413) catalyst provided 1,4-BuD in 89% yield at 96 h (Table 2, entry 8), but the Re–Ir(*exL*, 413) catalyst showed higher selectivities to by-products such as *n*-butane and BuOH at 24–96 h than the Re–Pd(*exL*, 413) catalyst (Table 2, entries 9–11) and *n*-butane and BuOH became the major products at 96 h (Table 2, entry 11). According to previous reports, rhenium oxide-modified noble metal catalysts, such as Rh–ReO_x,^{18b–e,g} Ru–ReO_x,^{18k} Pt–ReO_x^{18i,j} and Ir–ReO_x,^{18a,f,h,l,m} were effective for the hydrogenolysis of C–O bonds in glycerol,^{18a,b,f,h–l}

Table 1 Effect of the reduction methods on SUC hydrogenation over Re–Pd/SiO₂ and Re/SiO₂ catalysts

Entry	Catalyst	Conv./%	Selectivity/%					v^a /mmol g _{cat} ⁻¹ h ⁻¹
			GBL	1,4-BuD	THF	BA	BuOH	
1	Re–Pd(<i>inL</i> , 413)	3.9	94	1.8	0.0	3.8	0.0	0.8
2	Re–Pd(<i>G</i> , 473)	10	94	5.1	0.0	0.8	0.0	2.2
3	Re–Pd(<i>exL</i> , 413)	26	96	3.0	0.0	0.9	0.3	5.4
4	Re(<i>inL</i> , 413)	<1	—	—	—	—	—	<0.2
5	Re(<i>G</i> , 473)	<1	—	—	—	—	—	<0.2
6	Re(<i>exL</i> , 413)	7.0	94	3.9	0.0	1.6	0.9	1.5

SUC, succinic acid; GBL, γ -butyrolactone; 1,4-BuD, 1,4-butanediol; THF, tetrahydrofuran; BA, butyric acid; BuOH, 1-butanol. Reaction conditions: 5 wt% SUC solution 20 g (SUC 1 g, 1,4-dioxane 19 g), catalyst (Re = 14 wt%, Re/Pd = 8) amount 0.1 g, reaction temperature 413 K, H₂ pressure 8.0 MPa, reaction time 4 h. ^a Averaged conversion rate.

Table 2 Results of SUC hydrogenation over various M''-M'/SiO₂ catalysts

Entry	M''-M' catalyst	Time/h	Conv./%	Selectivity/%						$v^a/\text{mmol g}_{\text{cat}}^{-1} \text{h}^{-1}$	
				GBL	1,4-BuD	THF	BA	BuOH	<i>n</i> -Butane		Others
1	Pd(<i>exL</i> , 413) ^b	4	<1	—	—	—	—	—	—	—	<0.2
2	Re(<i>exL</i> , 413)	4	7.0	94	3.9	0.0	1.6	0.9	0.0	0.0	1.5
3	Re-Ru(<i>exL</i> , 413)	4	12	95	2.0	0.0	2.1	0.7	0.0	0.0	2.5
4	Re-Rh(<i>exL</i> , 413)	4	22	94	3.0	0.0	2.4	0.8	0.0	0.0	4.6
5	Re-Pd(<i>exL</i> , 413)	4	26	96	3.0	0.0	0.9	0.3	0.0	0.0	5.4
6	Re-Ir(<i>exL</i> , 413)	4	33	88	6.4	0.3	4.2	1.5	0.0	0.0	7.0
7	Re-Pt(<i>exL</i> , 413)	4	21	94	2.9	0.0	2.7	0.7	0.0	0.0	4.4
8	Re-Pd(<i>exL</i> , 413)	96	100	3.1	89	0.2	0.0	7.6	0.0	0.0	—
9	Re-Ir(<i>exL</i> , 413)	24	>99	56	27	0.7	2.0	12	1.6	1.0	—
10	Re-Ir(<i>exL</i> , 413)	48	100	4.0	32	1.2	0.0	54	6.8	1.7	—
11	Re-Ir(<i>exL</i> , 413)	96	100	0.1	0.0	0.7	0.0	22	60	17	—
12	Ti-Pd(<i>exL</i> , 413) ^c	4	<1	—	—	—	—	—	—	—	<0.2
13	W-Pd(<i>exL</i> , 413) ^c	4	<1	—	—	—	—	—	—	—	<0.2
14	Mo-Pd(<i>exL</i> , 413) ^c	4	0	—	—	—	—	—	—	—	0
15	Re(<i>exL</i> , 413) + Pd(<i>exL</i> , 413) ^d	4	3.0	>99	—	—	—	—	—	—	0.6

SUC, succinic acid; GBL, γ -butyrolactone; 1,4-BuD, 1,4-butanediol; THF, tetrahydrofuran; BA, butyric acid; BuOH, 1-butanol; Others, methane and ethane. Reaction conditions: 5 wt% SUC solution 20 g (SUC 1 g, 1,4-dioxane 19 g), catalyst amount 0.1 g (M'' = 14 wt%, M''/M' = 8, M' = Ru, Rh, Pd, Ir and Pt, M'' = Re, Mo, W and Ti; support = SiO₂), reaction temperature 413 K, H₂ pressure 8.0 MPa. ^a Averaged conversion rate. ^b Pd = 1 wt%. ^c Pd = 1 wt%, M''/Pd = 8. ^d Physical mixture of ReO_x/SiO₂ (0.1 g) and Pd/SiO₂ (0.1 g) catalysts.

tetrahydrofurfuryl alcohol^{18d,e,g} and so on in the aqueous phase. In addition, it is characteristic that Ir-ReO_x with high molar ratios of Re to Ir such as Re/Ir = 1–3 showed high activity in glycerol hydrogenolysis^{18a} compared to the case of Rh-ReO_x.^{18b-d} This tendency suggests that the combination of Re with Ir at high molar ratios of Re/Ir can result in high activity for hydrogenolysis of C–O bonds compared to the combination with other noble metals. It should be noted that Ir-ReO_x-based catalysts were effective in the formation of monoalcohols and alkanes from cellulose,^{19b,c,f} hemi-cellulose,^{19d,f} sugar alcohols,^{19a,f} and sugars^{19e,f} by the hydrogenolysis of multiple C–O bonds. In fact, the main products obtained for the Re-Ir(*exL*, 413) catalyst in SUC hydrogenation were strongly influenced by the reaction time, and the main product changed from shorter to longer reaction time as follows: GBL → 1,4-BuD → BuOH → *n*-butane. The reaction route of 1,4-BuD → BuOH → *n*-butane is due to C–O hydrogenolysis. In contrast, it has been reported that Pd-ReO_x showed no activity in glycerol hydrogenolysis at 393 K,^{18a} and this property can be connected to the high selectivity to 1,4-BuD in the hydrogenation of SUC. These results indicate that the Pd metal is a suitable additive for the synthesis of 1,4-BuD by hydrogenation of SUC. In addition, Ti-Pd, W-Pd and Mo-Pd catalysts showed no activity for the hydrogenation of SUC (Table 2, entries 12–14), which indicates that Re species are essential for the reaction. Taking into consideration that the Pd(*exL*, 413) catalyst showed no activity, it is concluded that Re species are the main active species on the Re-Pd catalysts for the reaction. Moreover, the physical mixture of Re(*exL*, 413) and Pd(*exL*, 413) catalysts (weight ratio of Re(*exL*, 413)/Pd(*exL*, 413) = 1) showed much lower activity than the Re-Pd(*exL*, 413) catalyst (Table 2, entries 5 and 15), suggesting that the high activity of the Re-Pd(*exL*, 413) catalyst can be caused by Re species and Pd species on the same support. Therefore,

the Re-Pd(*exL*, 413) catalyst was determined to be the suitable catalyst for the hydrogenation of SUC to 1,4-BuD under the reaction conditions ($T = 413 \text{ K}$, $P_{\text{H}_2} = 8 \text{ MPa}$). In addition, the Re and Pd amounts on the Re-Pd(*exL*, 413) catalyst were optimized by changing the molar ratio of Re/Pd, which resulted in the Re-Pd(*exL*, 413) catalyst with Re = 14 wt% and Pd = 1 wt% (Re/Pd molar ratio = 8) being the most preferable for the reaction (Fig. S1 and S2 in the ESI†). The optimized Re-Pd/SiO₂ catalyst in the hydrogenation of SUC is the same as that in the hydrogenation of STA.^{11,12}

Hydrogenation of various carboxylic acids over Re-Pd catalysts with different reduction methods

The hydrogenation of several dicarboxylic acids and related compounds was studied under the conditions of 413 K, 8 MPa H₂ and 4 h using Re-Pd catalysts (Re = 14 wt%, Pd = 1 wt%) (Table 3). In the case of the reactions of SUC (C4) and glutaric acid (GLU, C5) over the Re-Pd(*exL*, 413) catalyst, the corresponding lactone was produced with high selectivity (Table 3, entries 1 and 3). On the other hand, in the case of adipic acid (ADI, C6) and suberic acid (SUB, C8) over the Re-Pd(*exL*, 413) catalyst, the corresponding terminal-hydroxyl carboxylic acid (HCA) was produced with high selectivity (Table 3, entries 4 and 6). However, the reactivity of the dicarboxylic acids decreased with increasing carbon number of dicarboxylic acids (Table 3, entries 1, 3, 4 and 6). On the other hand, in the case of monocarboxylic acids (hexanoic acid (HXA, C6), octanoic acid (OCA, C8), STA (C18)), such a drastic decrease in reactivity with respect to the carbon number was not observed (Table 3, entries 8, 11 and 12). In addition, it was also confirmed that the concentration of the monocarboxylic acid HXA did not influence its averaged conversion rate strongly (Table 3, entry 10). These results indicate that

Table 3 Hydrogenation of several carboxylic acids and related compounds over Re-Pd(*exL*, 413) and Re-Pd(*inL*, 413) catalysts

Entry	Substrate	Carbon number	Catalyst	Conv./%	Selectivity/%					v^a /mmol g _{cat} ⁻¹ h ⁻¹
					Lactone	HCA	Diol	Monoalcohol	Others	
1	SUC	4	Re-Pd(<i>exL</i> , 413)	26	96	—	3.0	0.3	0.9	5.4
2			Re-Pd(<i>inL</i> , 413)	3.9	94	—	1.8	0.0	3.8	0.8
3	GLU	5	Re-Pd(<i>exL</i> , 413)	22	93	3.2	3.1	0.0	0.6	4.1
4	ADI	6	Re-Pd(<i>exL</i> , 413)	15	3.6	82	11	0.5	2.8	2.6
5			Re-Pd(<i>inL</i> , 413)	1.4	9.5	82	8.7	0.0	0.0	0.2
6 ^b	SUB	8	Re-Pd(<i>exL</i> , 413)	5.0	—	95	5.4	0.0	0.0	0.7
7 ^b			Re-Pd(<i>inL</i> , 413)	1.7	—	95	5.5	0.0	0.0	0.2
8	HXA	6	Re-Pd(<i>exL</i> , 413)	31	—	—	—	99	0.5	6.6
9			Re-Pd(<i>inL</i> , 413)	28	—	—	—	99	1.0	6.2
10	HXA ^c	6	Re-Pd(<i>exL</i> , 413)	19	—	—	—	99	1.4	8.0
11	OCA	8	Re-Pd(<i>exL</i> , 413)	44	—	—	—	96	3.7	7.7
12 ^d	STA	18	Re-Pd(<i>exL</i> , 413)	46	—	—	—	97	3.0	3.9
13 ^d			Re-Pd(<i>inL</i> , 413)	53	—	—	—	96	3.6	4.5
14	GBL	4	Re-Pd(<i>exL</i> , 413)	26	—	—	94	5.8	0.0	7.7
15	DVL	5	Re-Pd(<i>exL</i> , 413)	51	—	2.9	95	1.7	0.0	13
16	2-HBA	4	Re-Pd(<i>exL</i> , 413)	8.4	—	—	92	1.2	7.2	1.9
17	DMS	6	Re-Pd(<i>exL</i> , 413)	10	61	0.0	33	5.3	0.0	1.6
18	DVL + SUC	5/4	Re-Pd(<i>exL</i> , 413)	22 (SUC) 2.4 (DVL)	95 —	0.0 0	3.7 100	0.2 0.0	1.0 0.0	4.7 0.6

HCA, hydroxycarboxylic acid; Others, monocarboxylic acid, gas products and heavy products; SUC, succinic acid; GLU, glutaric acid; ADI, adipic acid; SUB, suberic acid; HXA, hexanoic acid; OCA, octanoic acid; STA, stearic acid; GBL, γ -butyrolactone; DVL, δ -valerolactone; 2-HBA, 2-hydroxybutyric acid; DMS, dimethyl succinate. Reaction conditions: substrate 1 g, 1,4-dioxane 19 g, Re-Pd(*exL*, 413) (Re = 14 wt%, Re/Pd = 8) 0.1 g, temperature 413 K, initial H₂ pressure 8 MPa, reaction time 4 h. ^a Averaged conversion rate. ^b Carbon balance = 80–90%. ^c HXA 2 g. ^d The data are referred from ref. 11.

the carbon number of carboxylic acids affected the reactivity only in the case of dicarboxylic acids. The decrease of the averaged conversion rate in the hydrogenation of dicarboxylic acids can be connected to the structure or adsorption state of dicarboxylic acids.

The activity of the Re-Pd(*exL*, 413) catalyst (Table 3, entries 1, 4 and 6) was compared with that of the Re-Pd(*inL*, 413) catalyst (Table 3, entries 2, 5 and 7) in the hydrogenation of dicarboxylic acids such as SUC (C4), ADI (C6) and SUB (C8). The Re-Pd(*exL*, 413) catalyst showed higher activity than the Re-Pd(*inL*, 413) catalyst regardless of the carbon number of dicarboxylic acids, which supports that *ex situ* liquid-phase reduction (*exL*) is effective for the Re-Pd/SiO₂ catalyst in the hydrogenation of dicarboxylic acids. On the other hand, in the case of hydrogenation of C6 and C18 monocarboxylic acids (Table 3, entries 8, 9, 12 and 13 (11)), the activity of the Re-Pd(*exL*, 413) catalyst was comparable to that of the Re-Pd(*inL*, 413) catalyst, indicating that the effect of the carbon number is small in the hydrogenation of monocarboxylic acids. Therefore, the reduction state of the catalyst will be largely dependent on the existence of dicarboxylic acids, and the two carboxylic acid groups in the dicarboxylic acids may suppress the reduction of the catalyst.

Hydrogenation of related compounds such as lactones and α -hydroxycarboxylic acid was also studied using the Re-Pd(*exL*, 413) catalyst (Table 3, entries 14–16). The lactones (GBL (C4) and δ -valerolactone (DVL, C5)) showed higher reactivity (Table 3, entries 14 and 15) than the corresponding dicarboxylic acids (Table 3, entries 1 and 3) to provide diols with high selectivity ($\geq 94\%$). In our previous work,¹² methyl

stearate was less reactive than the corresponding stearic acid over the Re-Pd(*inL*, 413) catalyst. To clarify the reason why the lactone, a cyclic ester, is reactive over the Re-Pd(*exL*, 413) catalyst, dimethyl succinate (DMS) was applied to the reaction over the Re-Pd(*exL*, 413) catalyst, giving lower reactivity than SUC (Table 3, entry 17). Therefore, the high reactivity of lactones can be attributed not to the difference in the reduction method but to the strain and/or accessibility of the cyclic structure. On the other hand, 2-hydroxybutyric acid (2-HBA) as a model substrate of hydroxycarboxylic acid (HCA) showed lower reactivity than lactones and simple carboxylic acids (Table 3, entry 16).

The time dependence in the hydrogenation of SUC and ADI over the Re-Pd(*exL*, 413) catalyst was investigated (Fig. 1, Table S2 in the ESI†). In the case of SUC hydrogenation, GBL was produced as an intermediate first and the highest GBL yield (85%) was obtained at a reaction time of 24 h. GBL was subsequently hydrogenated to 1,4-BuD and the highest 1,4-BuD yield (89%) was obtained at a reaction time of 96 h. The selectivity to BuOH increased after GBL was consumed (selectivity to GBL <1.0% at 96 h). Production of 4-hydroxybutyric acid was not observed at all. Therefore, the hydrogenation of SUC to 1,4-BuD proceeds by two consecutive reactions (Scheme 1(A)): (i) hydrogenation of SUC to GBL and (ii) hydrogenation of GBL to 1,4-BuD. Another important point is that the rate of the subsequent hydrogenation to 1,4-BuD is not as high as that of SUC hydrogenation, although the reactivity of GBL is higher than that of SUC as shown in Table 3. To clarify the cause of the low reactivity of GBL, the hydrogenation of the mixture of SUC and DVL was

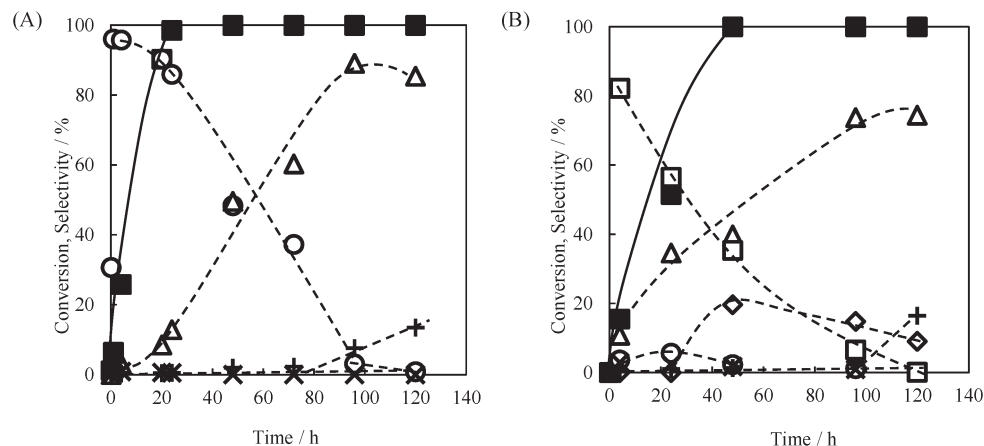
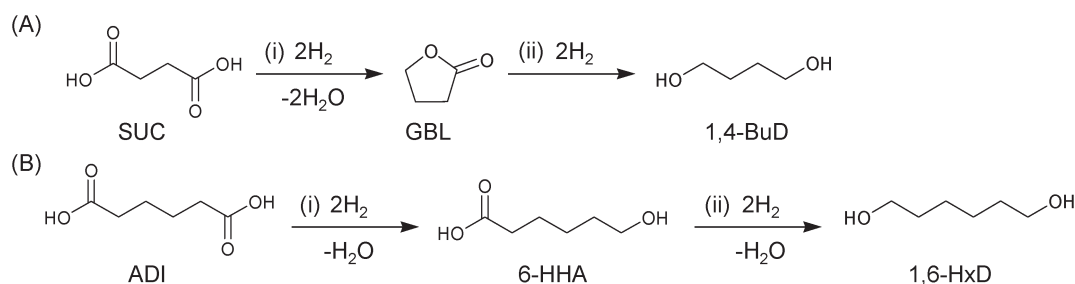


Fig. 1 Reaction time dependence in the hydrogenation of (A) SUC and (B) ADI over the Re–Pd(exL, 413) (Re/Pd = 8) catalyst. Reaction conditions: SUC or ADI 1 g, 1,4-dioxane 19 g, catalyst amount 0.1 g, reaction temperature 413 K, H₂ pressure 8.0 MPa. (A) ■: conversion; ○: γ -butyrolactone; Δ : 1,4-butanediol; \times : butyric acid; +: 1-butanol. (B) ■: conversion; □: 6-hydroxyhexanoic acid; ○: ϵ -caprolactone; Δ : 1,6-hexanediol; \times : hexanoic acid; +: 1-hexanol; \diamond : others. SUC, succinic acid; ADI, adipic acid. The data were obtained through independent experiments at different reaction times.



Scheme 1 The reaction routes of (A) SUC hydrogenation and (B) ADI hydrogenation.

investigated (DVL + SUC, Table 3, entry 18). It is demonstrated that the reactivity of DVL drastically decreases in the presence of SUC. These results suggest that hydrogenation of GBL on the Re–Pd(exL, 413) catalyst was suppressed by the presence of SUC, which can explain the behavior of the reaction time dependence (Fig. 1A). This result may be explained by the stronger adsorption of the carboxylic acid than the lactone, and a similar tendency was observed in our previous work on hydrogenation of carboxylic acids, where hydrogenolysis of alcohols was drastically suppressed in the presence of carboxylic acids.¹¹ On the other hand, in the case of ADI hydrogenation, 6-hydroxyhexanoic acid (6-HHA) was mainly produced as an intermediate with 82% selectivity at the initial reaction time of 4 h. The selectivity to 6-HHA decreased with increasing reaction time after the reaction time of 4 h, and the selectivity to 1,6-HxD increased. The highest 1,6-HxD yield of 74% was achieved at a reaction time of 96 h. Therefore, the hydrogenation of ADI to 1,6-HxD proceeds by two consecutive reactions (Scheme 1(B)): (i) hydrogenation of ADI to 6-HHA and (ii) hydrogenation of 6-HHA to 1,6-HxD. Judging from the selectivity to 1,6-HxD at low ADI conversion, the hydrogenation of 6-HHA to 1,6-HxD was not suppressed by the presence of ADI in comparison with the hydrogenation of SUC. In addition, hydrogenation of GLU provided DVL as an intermediate first and then a high yield of 1,5-pentanediol (71%) was obtained in 120 h (Table S2 in the ESI[†]). In previ-

ous studies, in the hydrogenation of GLU and ADI, Ru-based catalysts such as Ru(2 wt%)–Sn(2.35 wt%)/Al₂O₃ (ref. 6c) and Ru(5 wt%)–Sn(3 wt%)–Re(5 wt%)/C (ref. 6l) also gave high yields of 1,5-pentanediol (Ru–Sn/Al₂O₃: 75.6% and Ru–Sn–Re/C: 98%) and 1,6-HxD (Ru–Sn/Al₂O₃: 89.4% and Ru–Sn–Re/C: 96%) under the conditions of $T = 453$ – 523 K and $P_{\text{H}_2} = 6.5$ – 15 MPa. Therefore, these results indicate that the Re–Pd(exL, 413) catalyst can selectively hydrogenate dicarboxylic acids to diols in high yields (71–89%) under relatively mild conditions ($T = 413$ K, $P_{\text{H}_2} = 8$ MPa).

To ascertain whether the reaction proceeds on the surface of the Re–Pd catalyst, a leaching test was conducted. The hydrogenation of SUC was carried out under the same reaction conditions for 1 h to achieve 6.4% conversion, and then the catalyst was removed from the reaction mixture by filtration (Fig. S3 in the ESI[†]). The filtrate was heated again at 8 MPa H₂ for 2 h. The SUC hydrogenation reaction with the filtrate did not proceed further. These results indicate that SUC hydrogenation is catalyzed by the heterogeneous Re–Pd catalyst. On the other hand, the leaching amount of Re and Pd after the reaction (4 h) was found to be 3.5% and 0.4%, respectively, by using inductively coupled plasma atomic emission spectrometry (ICP-AES). The reusability of the catalyst was also tested (Table S3 in the ESI[†]). The method was similar to that for STA hydrogenation,¹¹ and the detailed method is described in the ESI[†]. The averaged conversion rate (v)

decreased with increasing number of uses, while high selectivity was maintained. The degree of activity decrease in SUC hydrogenation is larger than that in STA hydrogenation.¹¹ The leaching amount of Re and Pd species in SUC hydrogenation was larger than that in STA hydrogenation. At present, the decrease in averaged conversion rate is due to not only leaching of the Re species but also structural changes in the active sites because the structures of the active sites are sensitive to reduction conditions as discussed in the following section. Further investigation into the catalyst reuse method is necessary for this catalyst system.

Kinetic studies of hydrogenation of various dicarboxylic acids

The effect of reaction temperature on the hydrogenation of SUC over the Re–Pd(exL, 413) (Re/Pd = 8) catalyst was investigated. The results are listed in Table 4. The averaged conversion rate of the Re–Pd(exL, 413) catalyst increased with increasing reaction temperature, while the high selectivity to GBL ($\geq 96\%$) was maintained at any reaction temperature. The maximum 1,4-BuD yields over the Re–Pd(exL, 413) catalyst at 413, 433 and 453 K were obtained by reaction time optimization and were determined to be 89, 84 and 74%, respectively (entries 6–8). These results indicate that the maximum 1,4-BuD yield decreased with increasing reaction temperature. In addition, the quasi-formation rates of 1,4-BuD ($r_{1,4\text{-BuD}}$) from SUC at 413, 433 and 453 K, which were calculated on the basis of the metal loading amount, were 0.9, 2.3 and 5.3 h⁻¹, respectively. The quasi-formation rates over Re₂O₇ (483 K, 25 MPa H₂),^{6a} Re(3.6 wt%)-Pd(2 wt%)/TiO₂ (433 K, 15 MPa)^{6h} and Pd(1 wt%)-Re(4 wt%)/TiO₂ (473 K, 6.9 MPa, liquid-flow reaction)^{6j} are also listed in Table 4. The Re–Pd(exL, 413) catalyst showed a similar or higher quasi-formation rate under milder conditions, compared with the reported catalysts.

The reaction kinetics of hydrogenation of SUC over the Re–Pd(exL, 413) and Re(exL, 413) catalysts, which have the

same Re loading amount, and the kinetics of hydrogenation of ADI and GLU over the Re–Pd(exL, 413) catalyst were investigated. The results were obtained under the conditions where the conversion of the substrate was below 30%. Fig. 2 shows the effect of dicarboxylic acid (SUC, GLU and ADI) concentration on the activity of Re–Pd(exL, 413) and Re(exL, 413) catalysts. The effect was investigated by changing the amount of 1,4-dioxane and dicarboxylic acids (concentration: 3 to 30 wt%), and the detailed results are listed in Table S4 in the ESI.† The reaction orders with respect to the SUC concentration over the Re–Pd(exL, 413) and Re(exL, 413) catalysts were estimated to be +0.1 and +0.4, respectively, suggesting that SUC is more strongly adsorbed on the Re–Pd(exL, 413) catalyst than on the Re(exL, 413) catalyst. The presence of Pd can

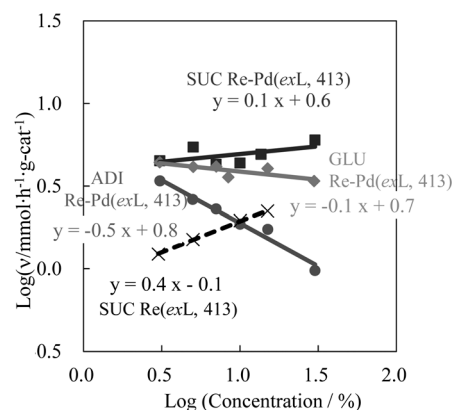


Fig. 2 Effect of substrate concentration on the hydrogenation of succinic acid (SUC), glutaric acid (GLU) and adipic acid (ADI) over the Re–Pd(exL, 413) (Re/Pd = 8) and Re(exL, 413) catalysts. Reaction conditions: 3–30 wt% dicarboxylic acid solution, 1,4-dioxane solvent 5.7–20 g, dicarboxylic acid 0.60–1.0 g, catalyst 0.060–0.10 g, reaction temperature 413 K, H₂ pressure 8.0 MPa, reaction time 4 h. The detailed data are shown in Table S4.† ■: SUC (Re–Pd(exL, 413)); ◆: GLU (Re–Pd(exL, 413)); ●: ADI (Re–Pd(exL, 413)); ×: SUC (Re(exL, 413)). v: averaged conversion rate.

Table 4 Effect of reaction temperature on SUC hydrogenation over the Re–Pd(exL, 413) catalyst

Entry	Catalyst	Temp./K	H ₂ /MPa	Time/h	Conv./%	Selectivity/%					v^a /mmol g _{cat} ⁻¹ h ⁻¹	$r_{1,4\text{-BuD}}^b$ /h ⁻¹
						GBL	1,4-BuD	THF	BA	BuOH		
1	Re–Pd(exL, 413)	373	8.0	4	2.0	97	3.2	0.0	0.0	0.0	0.4	—
2	Re–Pd(exL, 413)	393	8.0	4	6.6	97	2.4	0.0	0.9	0.0	1.4	—
3	Re–Pd(exL, 413)	413	8.0	4	26	96	3.0	0.0	0.9	0.3	5.4	—
4	Re–Pd(exL, 413)	433	8.0	2.5	31	97	1.4	0.0	1.1	0.4	11	—
5 ^c	Re–Pd(exL, 413)	453	8.0	2	34	97	1.2	0.4	1.1	0.4	30	—
6	Re–Pd(exL, 413)	413	8.0	96	100	3.1	89	0.2	0.0	7.6	—	0.9
7	Re–Pd(exL, 413)	433	8.0	36	100	7.3	84	0.3	0.0	8.6	—	2.3
8	Re–Pd(exL, 413)	453	8.0	14	100	7.0	74	1.3	0.0	18	—	5.3
9 ^d	Re ₂ O ₇	483	25	4	100	—	94	—	—	6.0	—	0.4
10 ^e	3.6 wt% Re–2 wt% Pd/TiO ₂	433	15	48	100	—	83	—	—	—	—	1.9
11 ^f	1 wt% Pd–4 wt% Re/TiO ₂	473	6.9	—	99	—	86	—	—	—	—	1.6

SUC, succinic acid; GBL, γ -butyrolactone; 1,4-BuD, 1,4-butanediol; THF, tetrahydrofuran; BA, butyric acid; BuOH, 1-butanol. Reaction conditions: SUC 1 g, 1,4-dioxane 19 g, catalyst 0.1 g (molar ratio of SUC (mol) to loading amount of total metal (mol) = 100) (entries 1–8). ^a Averaged conversion rate. ^b Quasi-formation rate of 1,4-BuD; calculated on the basis of the total metal loading amount. ^c Catalyst 0.05 g. ^d The data are listed from ref. 6a. Molar ratio of SUC (mol) to loading amount of total metal (mol) = 1.6. ^e The data are listed from ref. 6h. Molar ratio of SUC (mol) to loading amount of total metal (mol) = 110. ^f The data are listed from ref. 6j. This reaction was conducted under liquid flow (flow 5.6 mL h⁻¹, catalyst 4.12 g).

be connected to the enhancement of SUC adsorption on the catalyst surface, which was also supported by our previous work on the hydrogenation of STA using the Re–Pd(*inL*, 413) catalyst.¹¹ In addition, the reaction orders with respect to the initial GLU and ADI concentration over the Re–Pd(*exL*, 413) catalyst were estimated to be -0.1 and -0.5 , respectively. These results suggest that the dicarboxylic acids with longer alkyl chains on the catalyst surface can decrease the activity of the Re–Pd(*exL*, 413) catalyst, which can be connected to the lower reactivity of dicarboxylic acids with longer alkyl chains (Table 3, entries 6 and 8). One possible interpretation is that the carboxylic groups of the long dicarboxylic acids are easier to be adsorbed on the catalyst surface than those of the short dicarboxylic acids,²⁰ which suppresses the adsorption of H₂ by the effect of the bulkiness of dicarboxylic acids.

Fig. 3 shows the effect of H₂ pressure over the Re–Pd(*exL*, 413) and Re(*exL*, 413) catalysts using SUC, GLU and ADI as substrates, and the details are listed in Table S5 in the ESI.† The reactions were performed in the range from 2 MPa to 8 MPa H₂. The reaction orders with respect to H₂ pressure were estimated to be about +1 (+1.0 to +1.2) in all cases. The positive reaction orders indicate that the reaction rate was strongly influenced by H₂ pressure, meaning that the dissociation of H₂ or the reaction of the dissociated hydrogen species is involved in the rate-determining step. Considering that the dissociation of H₂ is very fast on the Pd or Re metal surface, the reaction of the dissociated hydrogen species will be the rate-determining step. According to our previous works,^{11,18,21} the reaction order of almost +1 with respect to H₂ pressure can be interpreted that hydrogen is heterolytically dissociated to proton (H⁺) + hydride (H⁻) on the Re–

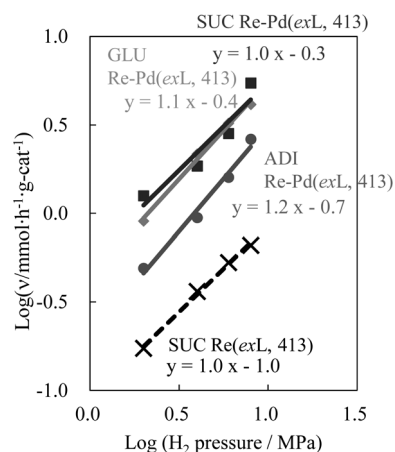


Fig. 3 Effect of H₂ pressure on the hydrogenation of succinic acid (SUC), glutaric acid (GLU) and adipic acid (ADI) over the Re–Pd(*exL*, 413) (Re/Pd = 8) and Re(*exL*, 413) catalysts. Reaction conditions: 5 wt% dicarboxylic acid solution 20 g (dicarboxylic acid 1 g, 1,4-dioxane 19 g), catalyst amount 0.1 g, reaction temperature 413 K, reaction time 4 h (Re(*exL*, 413) 16 h), H₂ pressure 2–8 MPa. The detailed data are shown in Table S5.† ■: SUC (Re–Pd(*exL*, 413)); ◆: GLU (Re–Pd(*exL*, 413)); ●: ADI (Re–Pd(*exL*, 413)); ×: SUC (Re(*exL*, 413)). *v*: averaged conversion rate.

Pd(*exL*, 413) catalyst and that the produced hydride is the active species for the hydrogenation of SUC.¹¹

Characterization of Re–Pd and related catalysts with different reduction methods

Various characterization techniques (XRD, XPS and XAFS) were applied to the catalysts in order to compare the structures of the Re–Pd/SiO₂ catalysts with different reduction methods (*exL*, *inL*, G).

Fig. 4 shows the XRD patterns of Re–Pd and Re catalysts with different reduction methods. The sharp peaks at 20.2°, 26.3° and 31.6° observed in Fig. 4d can be assigned to SUC (ICDD 00-049-2106). The signal due to amorphous SiO₂ was observed around 20° in all XRD patterns. In our previous work,¹¹ the Re–Pd(*inL*, 413, Reaction) catalyst showed broad signals around 2θ = 40° in the hydrogenation of STA (Fig. S4d in the ESI†), which were assigned to Re⁰(HCP), Re⁰(FCC) and Pd⁰(FCC). We proposed that Re⁰ is one of the main components of the active species in the hydrogenation of STA. In the hydrogenation of SUC, the Re–Pd(*exL*, 413, Reaction) catalyst showed broad signals around 2θ = 40° and sharp signals assignable to Re⁰(HCP) at 2θ = 37.8, 40.6, 42.9, 56.9 and 67.6° (Fig. 4a). On the other hand, the Re–Pd(*inL*, 413, Reaction) catalyst showed very small signals around 40° (Fig. 4b). The Re–Pd(G, 413, Reaction) catalyst showed broad signals around 40° (Fig. 4c). In the hydrogenation of ADI, the Re–Pd(*exL*, 413, Reaction) catalyst also showed much stronger broad signals around 40° and sharp signals for Re⁰(HCP) than the Re–Pd(*inL*, 413, Reaction) catalyst (Fig. S4c and S5d in the ESI†), and this tendency is similar to that in the hydrogenation of SUC. As for the Re/SiO₂ catalysts, the Re(*exL*, 413, Reaction) catalyst also showed broad signals around 2θ = 40° and sharp signals for Re⁰(HCP) (Fig. 4d), but the Re(*inL*, 413, Reaction) catalyst hardly showed broad and sharp signals (Fig. 4e). The Re(G, 473, Reaction) catalyst also showed broad signals around 40° (Fig. 4f).

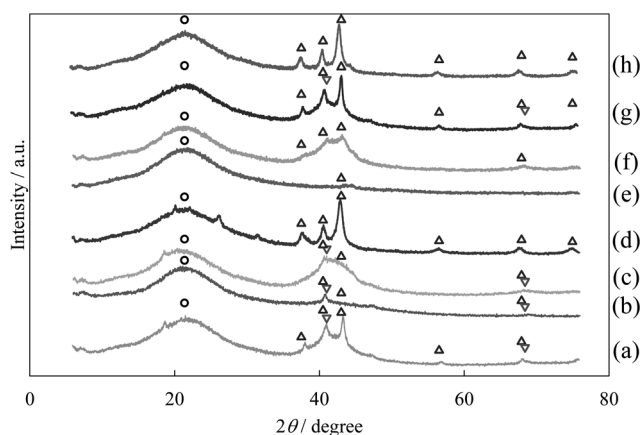


Fig. 4 XRD patterns of the Re–Pd (Re/Pd = 8) and Re catalysts after the reduction and the SUC reaction. (a) Re–Pd(*exL*, 413, Reaction), (b) Re–Pd(*inL*, 413, Reaction), (c) Re–Pd(G, 473, Reaction), (d) Re(*exL*, 413, Reaction), (e) Re (*inL*, 413, Reaction), (f) Re (G, 473, Reaction), (g) Re–Pd(*exL*, 413) and (h) Re(*exL*, 413). Reaction conditions are described in Table 1. Peak assignment: ○: SiO₂; △: Re(HCP); ▽: Pd.

On the other hand, a broad signal was observed around 40° over both Re–Pd(*inL*, 413, Reaction) and Re–Pd(*exL*, 413, Reaction) catalysts in the case of the hydrogenation of HXA and STA (Fig. S4e–h in the ESI†). Therefore, ReO_x species over the Re–Pd/SiO₂ catalyst were reduced by the *ex situ* liquid-phase reduction method, but not by the *in situ* liquid-phase reduction method in the hydrogenation of dicarboxylic acids, although the reduction of ReO_x species took place by the *in situ* liquid-phase reduction method in the hydrogenation of monocarboxylic acids. This result means that the reduction of ReO_x species was suppressed by the presence of dicarboxylic acids. In addition, no ReO_x species (ReO₂, ReO₃ and Re₂O₇) were observed in the range of 2θ = 20–30° for all the patterns, which indicates that ReO_x species were amorphous or highly dispersed on SiO₂. In order to clarify the state of the Re metal and Pd metal, the broad signals were fitted using the signals of Pd metal, Re⁰(HCP) and Re⁰(FCC) (Fig. S5 in the ESI†). The fitting analysis was conducted in a manner similar to that in our previous study.¹¹ The results of XRD fitting analysis are listed in Table 5. The particle sizes of Re⁰(HCP) on the *ex situ* liquid-phase reduced catalysts (8–9 nm) after the reaction are larger than those on the catalysts reduced with other methods (2–3 nm) (entries 1–6), and the larger Re⁰(HCP) particles were also observed on the catalysts after *ex situ* liquid-phase reduction (Fig. 4g and h and Table 5, entries 7 and 8). These results indicate that the *ex situ* liquid-phase reduction method can increase the particle size of Re⁰(HCP). Field emission scanning transmission electron microscopy (FE-STEM) and energy-dispersive X-ray (EDX) analysis of Re–Pd(*exL*, 413, Reaction) were also conducted (Fig. S6 in the ESI†). Similar to the TEM image of Re–Pd(*inL*, 413, Reaction) reported in the previous work,¹¹ small particles were observed in Fig. S6(A)† which seems to agree with the results of XRD analyses (Fig. 4 and Table 5), while large particles were not almost observed. In addition, from the TEM-EDX analysis, Re species were highly dispersed over the catalyst surface and were located near the Pd metal particles, suggesting some interactions between the ReO_x and Pd metal species.

In order to analyze the state of Re species on the catalyst surface, XPS analysis was conducted. Fig. 5, S7 and S8† and Table 6 show the results of XPS analyses for the Re(*exL*, 413, Reaction), Re(*exL*, 413), Re(*inL*, 413, Reaction), Re–Pd(*exL*, 413, Reaction),

Re–Pd(*exL*, 413) and Re–Pd(*inL*, 413, Reaction) catalysts. The only signals due to Pd 3d_{5/2} and 3d_{3/2} core levels were also observed at 335.1–335.3 and 340.5–340.7 eV, respectively (Fig. S7 in the ESI,† Table 6), for all the three reduced Re–Pd catalysts, and these signals can be assigned to Pd⁰ species.^{6g,i,11,22} Therefore, the Pd species on the surface of the catalysts was in the metallic state. Fig. 5 and S8† show the XPS profiles of the Re 4f region, and asymmetric signals were observed. The lines at 40.2–40.6, 41.2–41.6, 42.3–42.7 and 45.4–45.8 eV were assigned to Re⁰, Re³⁺, Re⁴⁺ and Re⁶⁺, respectively.^{6g,i,11,17,22–24} These XPS data were deconvoluted into these Re species in a manner similar to that in our previous study.¹¹ Table 6 lists the results of the deconvolution of the XPS data. In the case of the Re–Pd(*inL*, 413, Reaction) and Re(*inL*, 413, Reaction) catalysts, the signals can be almost deconvoluted into Re⁴⁺ and Re⁶⁺ species (area ratio of Re⁴⁺ + Re⁶⁺ to total Re >94%) (Fig. 5D and S8D,† Table 6, entries 1 and 4). On the other hand, in the case of the Re–Pd(*exL*, 413, Reaction) and Re(*exL*, 413, Reaction) catalysts, the signals can be deconvoluted into three components (Re⁰, Re³⁺ and Re⁴⁺) (Fig. 5F and S8F,† Table 6, entries 3 and 6), and the Re⁰ is the major species on the catalyst surface (area ratio of Re⁰ to total Re ≥58%). These results are supported by XRD analysis. In addition, in the case of the Re–Pd(*exL*, 413) and Re(*exL*, 413) catalysts, the signals can be deconvoluted into four components (Re⁰, Re³⁺, Re⁴⁺ and Re⁶⁺) (Fig. 5E and S8E,† Table 6, entries 2 and 5) and the contribution of Re⁰ and Re³⁺ was lower than that after the reaction. These results indicate that further reduction of the Re species proceeds slightly during the reaction.

XAS analyses were performed with the Re and Re–Pd catalysts after the reduction and SUC reaction. The Pd K-edge XANES patterns of all the catalysts were similar to that of the Pd foil (Fig. S9 in the ESI†), which indicates that the Pd species was reduced to the metallic state. This result was also verified by Pd K-edge EXAFS analysis (Fig. S10 and Table S6 in the ESI†). The formation of the Pd metal was also supported by the XPS results. Re L₃-edge XANES analyses of the Re–Pd and Re catalysts are shown in Fig. S11 in the ESI.† The average valence of the Re species can be estimated from the white line area in the Re L₃-edge XANES,²⁵ and the obtained average Re valence is listed in Table 7. The average valences of the Re–Pd(*inL*, 413, Reaction), Re–Pd(*exL*, 413,

Table 5 Results of the fitting analyses of the XRD patterns of Re–Pd and Re catalysts after reduction and SUC hydrogenation

Entry	Pattern (Fig.)	Catalyst	Size of Pd metal/nm	Size of Re metal (<i>d</i> _{Re})/nm		XRD area/10 ⁴ degree × counts		
				HCP	FCC	Total	Re ⁰ (HCP) (42.7°)	Re ⁰ (FCC) (40.0°)
1 ^a	4(a) and S5(a)	Re–Pd(<i>exL</i> , 413, Reaction)	7.2	8.9	1.8	17.3	5.0	12.3
2 ^a	4(b) and S5(a)	Re–Pd(<i>inL</i> , 413, Reaction)	11	1.7	1.4	3.2	1.6	1.6
3 ^a	4(c)	Re–Pd(G, 473, Reaction)	6.5	2.1	2.9	18.8	14.3	4.5
4 ^a	4(d)	Re(<i>exL</i> , 413, Reaction)	—	8.1	1.7	11.7	6.8	5.0
5 ^a	4(e)	Re(<i>inL</i> , 413, Reaction)	—	3.2	—	1.0	1.0	—
6 ^a	4(f)	Re(G, 473, Reaction)	—	2.6	3.3	16.0	12.5	3.5
7	4(g)	Re–Pd(<i>exL</i> , 413)	7.2	7.1	1.9	15.9	5.7	10.2
8	4(h)	Re(<i>exL</i> , 413)	—	8.5	1.8	9.1	5.8	3.2

^a Reaction conditions are described in Table 1.

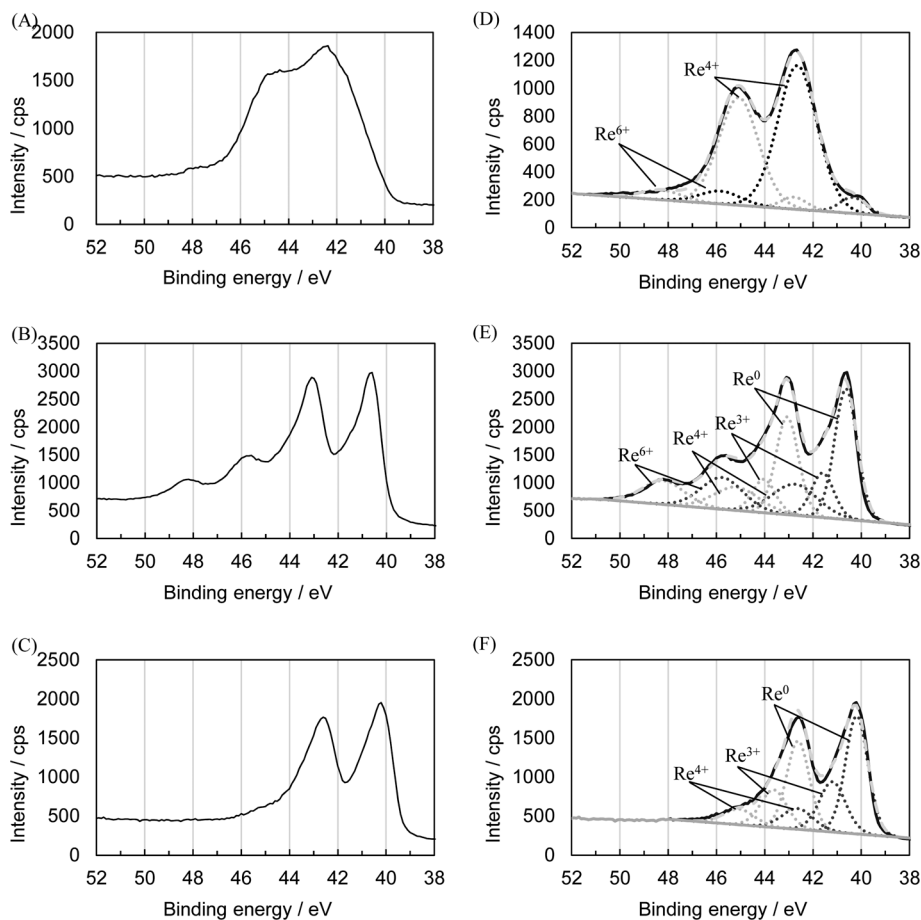


Fig. 5 The results of XPS for Re 4f over the Re-Pd catalysts ((A, D) Re-Pd(*inL*, 413, Reaction), (B, E) Re-Pd(*exL*, 413), (C, F) Re-Pd(*exL*, 413, Reaction)). (A–C): Raw data, (D–F): analysis results. Reaction conditions: 5 wt% SUC solution 20 g (SUC 1 g, 1,4-dioxane 19 g), catalyst amount 0.1 g, reaction temperature 413 K, H₂ pressure 8.0 MPa, reaction time 4 h. Black line: raw spectra; black dotted line: 4f_{7/2} for Re⁰, Re³⁺, Re⁴⁺ and Re⁶⁺; gray dotted line: 4f_{5/2} for Re⁰, Re³⁺, Re⁴⁺ and Re⁶⁺; gray broken line: the result of fitting; gray line: background. The fitted values are shown in Table 6.

Table 6 The results of XPS analyses of Re-Pd (Re/Pd = 8) and Re catalysts after reduction and SUC hydrogenation

Entry	Spectra (Fig.)	Catalyst	Re/Pd	Pd _s ⁰			Re _s ⁰			Re _s ³⁺			Re _s ⁴⁺			Re _s ⁶⁺			Re _{s,total} / Pd _s ⁰
				B.E. ^a /eV	B.E. ^b /eV	Area ratio/%	B.E. ^b /eV	Area ratio/%	B.E. ^b /eV	Area ratio/%	B.E. ^b /eV	Area ratio/%	B.E. ^b /eV	Area ratio/%					
1	S7A, 5A and 5D	Re-Pd(<i>inL</i> , 413, Reaction) ^c	8	335.1	—	—	—	—	42.3	95	45.8	4.9	52						
2	S7B, 5B and 5E	Re-Pd(<i>exL</i> , 413)	8	335.3	40.6	44	41.6	15	42.7	21	45.8	20	62						
3	S7C, 5C and 5F	Re-Pd(<i>exL</i> , 413, Reaction) ^c	8	335.2	40.2	58	41.2	29	42.6	14	—	—	34						
4	S8A and S8D	Re(<i>inL</i> , 413, Reaction) ^c	—	—	40.3	6.2	—	—	42.6	86	45.8	8.0	—						
5	S8B and S8E	Re(<i>exL</i> , 413)	—	—	40.4	41	41.4	16	42.5	27	45.4	16	—						
6	S8C and S8F	Re(<i>exL</i> , 413, Reaction) ^c	—	—	40.3	60	41.4	15	42.6	25	—	—	—						

^a B.E.: binding energy for Pd 3d_{5/2}. ^b B.E.: binding energy for Re 4f_{7/2}. ^c Reaction conditions: 5 wt% SUC solution 20 g (SUC 1 g, 1,4-dioxane 19 g), catalyst amount 0.1 g, reaction temperature 413 K, H₂ pressure 8.0 MPa, reaction time 4 h.

Reaction) and Re-Pd(G, 473, Reaction) catalysts were determined to be +3.7, +1.2 and +1.3, respectively (Table 7, entries 5, 7 and 8), which indicates that the degree of reduction of Re species on the Re-Pd(*exL*, 413, Reaction) and Re-Pd(G, 473, Reaction) catalysts is higher than that on the Re(*inL*, 413, Reaction) catalyst.

Fig. 6 and Table 7 show the results of Re L₃-edge EXAFS analysis of the Re and Re-Pd catalysts after the reduction and

SUC reaction. On these samples, Re=O, Re-O and Re-Re bonds were detected. In particular, the valence of Re can also be estimated approximately from the CN of Re=O and Re-O (valence of Re = 2 × CN_{Re=O} + 1 × CN_{Re-O}).^{11,18e,26} The calculated values of the Re valence from EXAFS analyses agreed well with the Re valence from Re L₃-edge XANES as listed in Table 7. It is verified that the local structure of the Re species on the *in situ* liquid-phase reduced catalysts was more oxidized than that on the *ex*

Table 7 Valence of Re determined from XANES analysis and curve fitting results for the Re L₃-edge EXAFS analysis of Re–Pd (Re = 14 wt%, Pd = 1 wt%) and Re (Re = 14 wt%) catalysts after reduction and SUC hydrogenation^a

Entry	Catalyst	Valence of Re ^b	Shells	CN ^c	$R^d/10^{-1}$ nm	$\sigma^e/10^{-1}$ nm	$\Delta E_0^f/eV$	$R_f^g/\%$
1 ^h	Re(<i>inL</i> , 413, Reaction)	3.8	Re=O	0.3	1.77	0.094	-15.0	6.3
			Re–O	3.3	2.06	0.096	3.4	
			Re–Re	1.3	2.60	0.076	-11.1	
2 ⁱ	Re(<i>exL</i> , 413)	1.6	Re=O	0.3	1.76	0.095	-12.0	1.9
			Re–O	1.1	2.07	0.093	6.3	
			Re–Re	7.4	2.73	0.060	-0.3	
3 ^h	Re(<i>exL</i> , 413, Reaction)	1.1	Re–O	1.1	2.08	0.093	9.5	2.6
			Re–Re	8.0	2.75	0.060	0.7	
			Re–O	1.6	2.06	0.092	5.2	
4 ^h	Re(G, 473, Reaction)	1.4	Re–Re	7.3	2.75	0.061	1.0	1.9
			Re=O	0.3	1.76	0.095	-15.0	
			Re–O	3.3	2.08	0.098	5.5	
5 ^h	Re–Pd(<i>inL</i> , 413, Reaction) Re/Pd = 8	3.7	Re–Re	1.4	2.60	0.060	-11.8	5.1
			Re=O	0.2	1.74	0.095	13.2	
			Re–O	1.5	2.04	0.095	4.9	
6 ⁱ	Re–Pd(<i>exL</i> , 413) Re/Pd = 8	1.6	Re–Re	7.2	2.70	0.095	-2.9	1.5
			Re=O	0.2	1.74	0.095	13.2	
			Re–O	1.5	2.04	0.095	4.9	
7 ^h	Re–Pd(<i>exL</i> , 413, Reaction) Re/Pd = 8	1.2	Re–O	1.1	2.13	0.099	15.4	4.7
			Re–Re	6.2	2.67	0.099	-7.2	
			Re–O	1.7	2.09	0.096	8.0	
8 ^h	Re–Pd(G, 473, Reaction) Re/Pd = 8 NH ₄ ReO ₄ Re powder	1.3	Re–Re	7.4	2.73	0.074	0.4	1.4
			Re=O	4	1.73	0.060	0.0	
			Re–O	1.7	2.09	0.096	8.0	
			Re–Re	12	2.74	0.060	0.0	

^a Fourier filtering range: 0.092–0.350 nm. ^b Valence of Re was determined from XANES analysis (Fig. S11). ^c Coordination number. ^d Bond distance. ^e Debye–Waller factor. ^f Difference in the origin of photoelectron energy between the reference and the sample. ^g Residual factor. ^h Reaction conditions: 5 wt% SUC solution 20 g (SUC 1 g, 1,4-dioxane 19 g), cat. 0.2 g, 413 K, 8 MPa, 2 h. ⁱ The catalysts were only reduced by the *ex situ* liquid-phase reduction method.

situ liquid-phase reduced catalysts, which is also supported by the results of XRD and XPS. The CN_{Re–Re} is determined by two factors: the molar ratio of Re metal to total Re species and the particle size of Re metal (Table S7 in the ESI†). The particle size of Re metal can be obtained from the XRD results (Table 4). Using these values, we determined the molar ratio of Re metal to total Re. The calculation of bulk and surface molar ratio of Re species was conducted using the results of the valence of bulk Re (XANES), the molar ratio of Reⁿ⁺ species (XPS) and the dispersion of Re⁰ particles (XRD). The calculation methods were also the same as those used in our previous report,¹¹ and the details are shown in the ESI (Table S7†). The order of the molar ratio of Re⁰ to total Re (Table S7†) is as follows: Re–Pd(G, 473, Reaction) (0.71) ≈ Re(*exL*, 413, Reaction) (0.69) ≈ Re–Pd(G, 473, Reaction) (0.64) ≈ Re–Pd(*exL*, 413, Reaction) (0.63) ≫ Re–Pd(*inL*, 413, Reaction) (0.11) ≈ Re(*inL*, 413, Reaction) (0.08), and this trend agreed with the XRD peak area due to the Re metal as listed in Table 5, assuming that the diffraction intensity of Re⁰(HCP) and Re⁰(FCC) is the same. Table 8 lists the estimation of the surface metal amount determined by the above catalyst characterization. The ratio of the Re³⁺ + Re⁴⁺ amount to the total surface metal amount ((Re³⁺ + Re⁴⁺)/(Pd_s⁰ + Re_s⁰); assuming that Re_sⁿ⁺ = Reⁿ⁺ because of the high dispersion) on the *ex situ* liquid-phase reduced catalysts (≈1) is much lower than that on the *in situ* liquid-phase reduced catalysts (>7) and is higher than that on the Re–Pd(G, 473, Reaction) catalyst (0.38). These results indicate that the degree of reduction of Re species on the *ex situ* liquid-phase reduced catalysts is located between those on the *in situ* liquid-phase reduced catalysts and gas-

phase reduced catalysts. In addition, the amount of Re_s⁰ species on the *in situ* liquid-phase reduced catalysts was much smaller than those on the other catalysts, which may lead to the low intensity or absence of the signal of Re⁰ species in the results of XPS analysis (Table 6). In our previous work, it was reported that the amount of CO adsorbed on the Re–Pd(G, 473) catalyst is lower than that of the calculated surface metals (Re_s⁰ + Pd_s⁰), suggesting that the surface of Re⁰ and Pd⁰ particles on the Re–Pd catalyst in STA hydrogenation was partially covered with Reⁿ⁺ species.¹¹ Therefore, it is suggested that, in the case of SUC hydrogenation, the surface of Re⁰ and Pd⁰ particles on the Re–Pd catalysts can be also partially covered with Reⁿ⁺ species. In our previous work, it was proposed that the catalytically active species on the Re–Pd(*inL*, 413) catalyst for hydrogenation of STA can be formed by the combination of Re⁰ with Reⁿ⁺.¹¹ Therefore, the species composed of Re⁰ with Reⁿ⁺ will be also a catalytically active one in the case of the hydrogenation of dicarboxylic acids. Suitable molar ratios of (Re³⁺ + Re⁴⁺)/Re_s⁰ or (Re³⁺ + Re⁴⁺)/(Pd_s⁰ + Re_s⁰) in terms of the generation of the active sites for hydrogenation of dicarboxylic acids can be obtained on the *ex situ* liquid-phase reduced catalysts. This interpretation is also supported by the previous results in the hydrogenation of STA (2.2) (Table 8, entry 9). In the case of the *in situ* reduced catalysts, the surface molar ratio of (Re³⁺ + Re⁴⁺)/(Re_s⁰ + Pd_s⁰) is very high (>7) (Table 8, entries 1 and 5), which leads to low activity because of the lack of Re⁰ species. In contrast, in the case of the Re–Pd(G, 473) catalyst, the ratio of Reⁿ⁺ to surface metals (0.38) was lower than those for the other catalysts (Table 8, entry 4), which also leads to low activity because of the lack of Reⁿ⁺

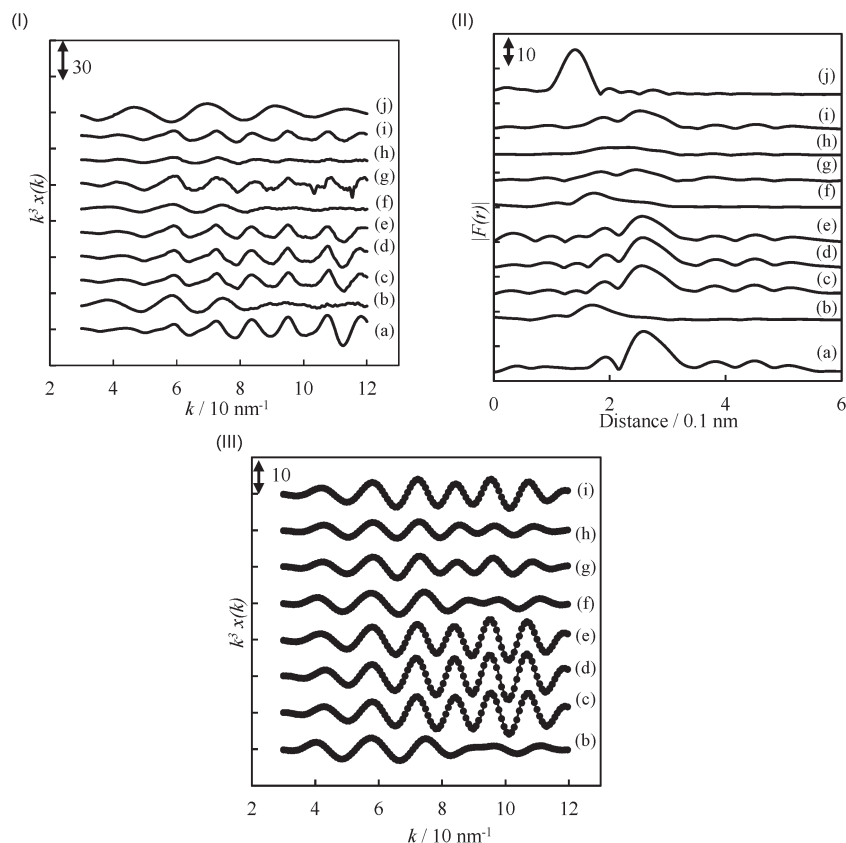


Fig. 6 Results of Re L_3 -edge EXAFS analysis of Re–Pd (Re/Pd = 8) and Re (Re = 14 wt%) catalysts after the reduction and SUC reaction. (I) k^3 -Weighted EXAFS oscillations. (II) Fourier transform of k^3 -weighted Re L_3 -edge EXAFS, FT range: 30–120 nm^{-1} . (III) Fourier filtered EXAFS data (solid line) and calculated data (dotted line), Fourier filtering range: 0.092–0.350 nm. (a) Re powder, (b) Re(*inL*, 413, Reaction), (c) Re(*exL*, 413), (d) Re(*exL*, 413, Reaction), (e) Re(G, 473, Reaction), (f) Re–Pd(*inL*, 413, Reaction), (g) Re–Pd (*exL*, 413), (h) Re–Pd(*exL*, 413, Reaction), (i) Re–Pd(G, 473, Reaction) and (j) Re_2O_7 .

Table 8 Estimation of the surface metal amount

Entry	Catalyst	Amount/mmol g_{cat}^{-1}							$\frac{\text{Re}^{3+} + \text{Re}^{4+}}{\text{Pd}_s^0 + \text{Re}_s^0}$	$v^d/\text{mmol } g_{\text{cat}}^{-1} \text{ h}^{-1}$	
		Pd_{total}	Pd_s^{0a}	Re_{total}	$\text{Re}(\text{HCP})_s^b$	$\text{Re}(\text{FCC})_s^b$	Re_s^{0c}	$\text{Pd}_s^0 + \text{Re}_s^0$			$\text{Re}^{3+} + \text{Re}^{4+}$
1	Re–Pd(<i>inL</i> , 413, Reaction)	0.094	0.0096	0.75	0.032	0.039	0.071	0.081	0.64	7.9	0.8
2	Re–Pd(<i>exL</i> , 413)	0.094	0.015	0.75	0.033	0.22	0.25	0.27	0.17	0.64	—
3	Re–Pd(<i>exL</i> , 413, Reaction)	0.094	0.016	0.75	0.021	0.26	0.28	0.29	0.27	0.94	5.4
4	Re–Pd(G, 473, Reaction)	0.094	0.015	0.75	0.26	0.060	0.32	0.34	0.13	0.38	2.2
5	Re(<i>inL</i> , 413, Reaction)	—	—	0.75	0.027	0.0	0.027	0.027	0.63	24	<0.2
6	Re(<i>exL</i> , 413)	—	—	0.75	0.048	0.13	0.17	0.17	0.20	1.2	—
7	Re(<i>exL</i> , 413, Reaction)	—	—	0.75	0.051	0.18	0.23	0.23	0.23	1.0	1.5
8	Re(G, 473, Reaction)	—	—	0.75	0.20	0.043	0.24	0.24	0.22	0.9	<0.2
9	Re–Pd(<i>inL</i> , 413, Reaction) ^e	0.094	0.017	0.75	0.12	0.064	0.19	0.20	0.42	2.2	4.5

^a The amount of surface Pd metal atoms [Pd_s^0] is calculated from both the dispersion (D) and total Pd metal atoms [$\text{Pd}_{\text{total}}^0$]. D was calculated from the XRD particle size (d_{XRD} , Table 5) by using the equation: d_{XRD} [nm] = 1.12 (Pd)/ D . ^b The amount is determined from the molar ratio described in Table S7. ^c $\text{Re}_s^0 = \text{Re}^0(\text{HCP})_s + \text{Re}^0(\text{FCC})_s$. ^d Averaged conversion rate at <30% conversion (Table 1). ^e The results for the catalyst after STA hydrogenation.¹¹

species. On the other hand, the Re(G, 473, Reaction) catalyst gave Re^0 species with a comparable amount to Re^{n+} species ($(\text{Re}^{3+} + \text{Re}^{4+})/(\text{Re}_s^0 + \text{Pd}_s^0) = 0.9$) (Table 8, entry 8). In our previous work, it was reported that the amount of Re metal on the surface of the Re(G, 473) catalyst is much lower than that on the Re–Pd(G, 473) catalyst from the results of CO adsorption amount of these catalysts,¹¹ suggesting that the surface Re metal species

is easily covered by ReO_x species. Therefore, the amount of the exposed Re metal on the catalyst will be decreased in this case, although the molar ratio of $(\text{Re}^{3+} + \text{Re}^{4+})/(\text{Pd}_s^0 + \text{Re}_s^0)$ was estimated to be about +1.

From the above catalyst characterization results and the discussion on the hydrogenation of dicarboxylic acids, the structures of the Re–Pd(*exL*, 413, Reaction), Re–Pd(*inL*, 413,

Reaction) and Re–Pd(G, 473, Reaction) catalysts (Fig. 7) and the reaction mechanism of hydrogenation of SUC over Re–Pd(exL, 413) are proposed (Scheme S1 in the ESI†). In the case of the Re–Pd(exL, 413, Reaction) catalyst, the particle size of Pd is 7.2 nm (Table 5) and the surface of Pd particles is partially covered with Reⁿ⁺ (Re³⁺ + Re⁴⁺). The amount ratio of Re⁰(HCP):Re⁰(FCC):Re³⁺:Re⁴⁺:Re⁶⁺ was estimated to be 18:45:25:12:0.0, and the main species of Re⁰ is fcc. The Re⁰ species form 1.8 nm Re⁰(FCC) particles and 8.9 nm Re⁰(HCP) particles. The model structure is depicted in Fig. 7(A) where the Re⁰(HCP) particles with a size of 8.9 nm were not included because of their small contribution. The surface of both Re⁰(HCP) and Re⁰(FCC) particles can be also partially covered with Reⁿ⁺ (Re³⁺ + Re⁴⁺) species ((Re³⁺ + Re⁴⁺)/(Pd_s⁰ + Re_s⁰) = 0.94). This structure is similar to the Re–Pd(inL, 413, Reaction) catalyst in the hydrogenation of STA (Fig. 7(B)).¹¹ On the other hand, in the case of the Re–Pd(inL, 413, Reaction) catalyst in the hydrogenation of dicarboxylic acids, the particle size of Pd is 11 nm (Table 5) and the surface of Pd particles is partially covered with Reⁿ⁺ (Re³⁺ + Re⁴⁺). The amount ratio of Re⁰(HCP):Re⁰(FCC):Re³⁺:Re⁴⁺:Re⁶⁺ was estimated to be 5.3:5.3:0.0:85:4.0, and the Re⁰ species was rather minor, although the Re⁰ species form 1.7 nm Re⁰(HCP) particles and 1.4 nm Re⁰(FCC) particles ((Re³⁺ +

Re⁴⁺)/(Pd_s⁰ + Re_s⁰) = 7.9) (Fig. 7(C)). Dicarboxylic acids suppress the reduction of Re species, although monocarboxylic acids do not. At present, the mechanism of the suppression of catalyst reduction by dicarboxylic acids is not elucidated, and further investigation into the interaction between the dicarboxylic acids and the Re (and Pd) species on the calcined catalyst is necessary. In the case of the Re–Pd(G, 473, Reaction) catalyst in the hydrogenation of dicarboxylic acids, the ratio of Re⁰(HCP):Re⁰(FCC):Re³⁺:Re⁴⁺:Re⁶⁺ was estimated to be 54:17:7.2:10:12, and the Re⁰ species form 2.1 nm Re⁰(HCP) particles and 1.9 nm Re⁰(FCC) particles. It is characteristic that the molar ratio of (Re³⁺ + Re⁴⁺)/(Pd_s⁰ + Re_s⁰) on the Re–Pd(G, 473, Reaction) catalyst is clearly lower than that on the Re–Pd(exL, 413, Reaction) catalyst (Fig. 7(D)). The ratio of (Re³⁺ + Re⁴⁺)/(Pd_s⁰ + Re_s⁰) can be dependent on the degree of reduction of Re species, and the medium level of ratio can be connected to the good performance of the Re–Pd(exL, 413, Reaction) catalyst considering that the catalytically active species consist of Re⁰ and Reⁿ⁺. From the kinetic studies, the main role of Reⁿ⁺ species is to promote the heterolytic dissociation of H₂ to produce reactive hydride species and protons at the interface between Re⁰ and Reⁿ⁺, and this role is also suggested by the results of STA hydrogenation on Re–Pd(inL, 413).¹¹ In addition, the role of Pd is to promote the reduction

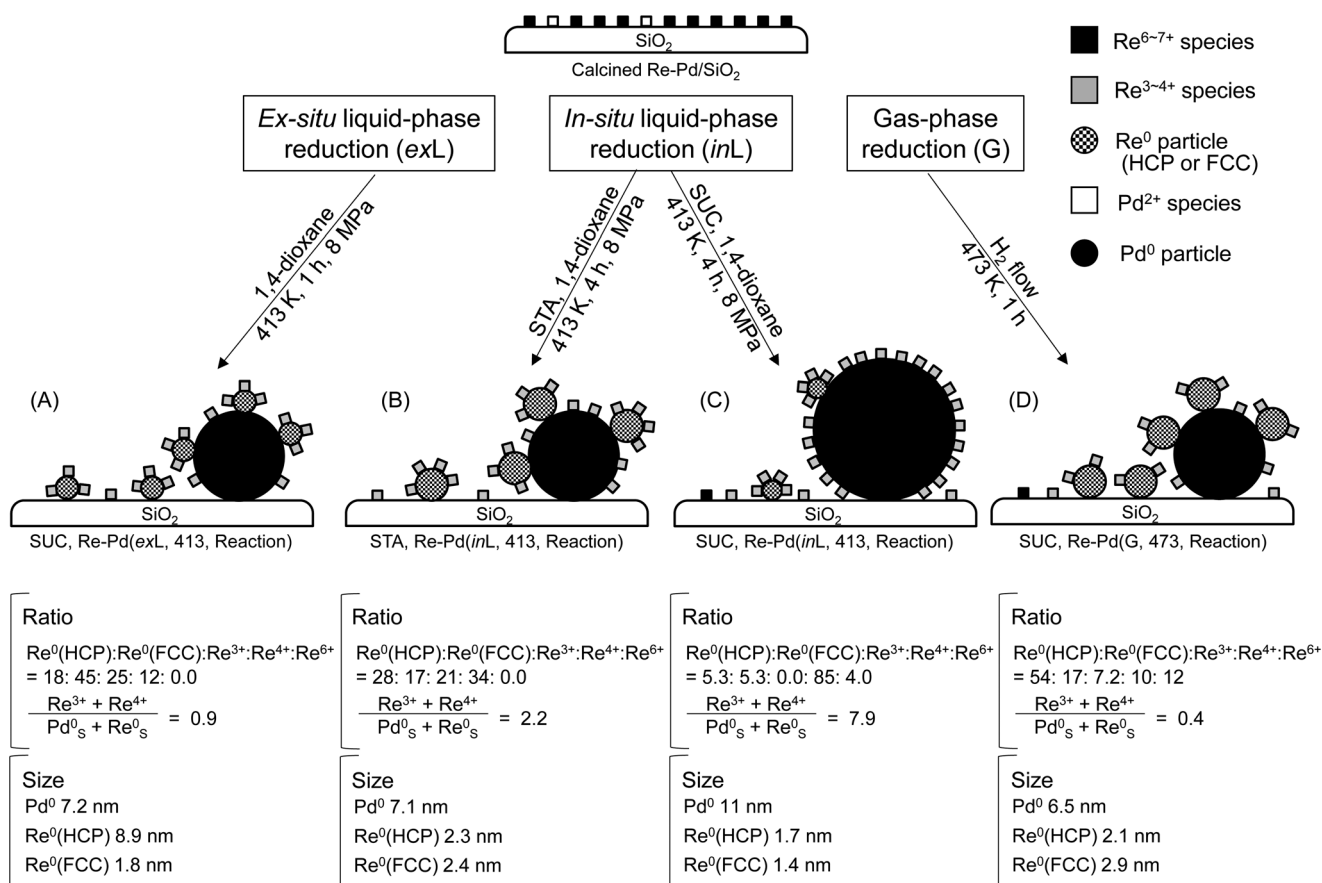


Fig. 7 Model structures of the Re–Pd/SiO₂ catalysts. (A) SUC hydrogenation, Re–Pd(inL, 413, Reaction); (B) STA hydrogenation, Re–Pd(inL, 413, Reaction);¹¹ (C) SUC hydrogenation, Re–Pd(exL, 413, Reaction); (D) SUC hydrogenation, Re–Pd(G, 473, Reaction). Particle sizes are listed in Table 5, and the ratios of the species are listed in Tables 8 and S7.†

of Re^{n+} to Re^0 and strengthen the interaction between the carboxyl group and the catalyst surface as suggested in our previous report on STA hydrogenation.¹¹ Scheme S1† illustrates the proposed reaction mechanism of hydrogenation of SUC to 1,4-BuD on the basis of the similarity of the reaction behavior to that of STA hydrogenation¹¹ and focuses on the role of Re^0 – Re^{n+} active sites, with the role of Pd not included. SUC or GBL are adsorbed on Re^0 near the Re^0 – Re^{n+} interface (step I, V), and then they are hydrogenated by the hydride species (step III, VII) which is produced from the heterolytic dissociation of H_2 at the interface (step II, VI).

Conclusions

The catalytic activity of Re – Pd/SiO_2 and Re/SiO_2 catalysts in the hydrogenation of dicarboxylic acids is influenced by the reduction methods. The *ex situ* liquid-phase reduction is more effective than the *in situ* liquid-phase and gas-phase reductions for the hydrogenation of dicarboxylic acids, while, for the hydrogenation of monocarboxylic acids, *in situ* liquid-phase reduction is also effective. High diol yields in the hydrogenation of dicarboxylic acids on the *ex situ* liquid-phase reduced catalysts are obtained and the diols are formed *via* lactones or hydroxycarboxylic acids as reaction intermediates. Catalyst characterization indicates that the *ex situ* liquid-phase reduced Re – Pd/SiO_2 has Pd^0 , $\text{Re}^0(\text{HCP})$, $\text{Re}^0(\text{FCC})$, Re^{3+} and Re^{4+} , and the surface metals (Pd^0 , $\text{Re}^0(\text{HCP})$, $\text{Re}^0(\text{FCC})$) can be covered with Re^{3+} and Re^{4+} species. These results of characterization are similar to those on the *in situ* liquid-phase reduced catalyst after hydrogenation of stearic acid. Considering that the combination of Re^0 species with Re^{n+} species has been proposed as the active site, it is suggested that the medium amount ratio of $\text{Re}^{n+}/(\text{Pd}_s^0 + \text{Re}_s^0)$ ($= 0.94$) such as that obtained in the *ex situ* reduced catalysts is suitable for hydrogenation of carboxylic acids. In addition, the amount of Re^{n+} species on the *in situ* liquid-phase reduced catalysts in the hydrogenation of dicarboxylic acids is much higher than that of surface Re^0 species. This result suggests that the presence of dicarboxylic acids suppresses the reduction of Re species on the catalysts to Re^0 which is an important component of active site, although that of monocarboxylic acids does not. This behavior explains the low activity of *in situ* liquid-phase reduced catalysts in the hydrogenation of dicarboxylic acids.

Acknowledgements

A part of this work is supported by the JSPS KAKENHI “Grant-in-Aid for Scientific Research (A)” (26249121) and “Grant-in-Aid for JSPS Fellows” (263554). We also appreciate the Technical Division of School of Engineering at Tohoku University for XPS measurements.

References

- (a) A. Corma, S. Iborra and A. Velty, *Chem. Rev.*, 2007, **107**, 2411–2502; (b) M. Besson, P. Gallezot and C. Pinel, *Chem. Rev.*, 2014, **114**, 1827–1870; (c) J. Pritchard, G. J. Filonenko, R. V. Putten, E. J. M. Hensen and E. A. Pidko, *Chem. Soc. Rev.*, 2015, **44**, 3803–3833; (d) D. Y. Murzin and I. L. Simakova, *Catal. Ind.*, 2011, **3**, 218–249; (e) Y. Nakagawa and K. Tomishige, *Catal. Sci. Technol.*, 2011, **1**, 179–190; (f) Y. Nakagawa, M. Tamura and K. Tomishige, *ACS Catal.*, 2013, **3**, 2655–2668; (g) Y. Nakagawa, M. Tamura and K. Tomishige, *J. Mater. Chem. A*, 2014, **2**, 6688–6702; (h) P. Gallezot, *Chem. Soc. Rev.*, 2012, **41**, 1538–1558; (i) W. Niu, K. M. Draths and J. W. Frost, *Biotechnol. Prog.*, 2002, **18**, 201–211.
- J. Akhtar, A. Idris and R. A. Aziz, *Appl. Microbiol. Biotechnol.*, 2014, **98**, 987–1000.
- I. Fukawa, *ARC Report, RS-978*, 2014, <https://www.asahi-kasei.co.jp/arc/service/pdf/978.pdf>, (accessed March 2016).
- Myriant Corporation, *Succinic Acid & Derivatives SBU*, <http://www.myriant.com/pdf/myriant-succinic-acid-customer-presentation-english.pdf>, (accessed February 2016).
- C. Delhomme, D. Weuster-Botz and F. E. Kühm, *Green Chem.*, 2009, **11**, 13–26.
- (a) H. S. Broadbent, G. C. Campbell, W. J. Bartley and J. H. Johnson, *J. Org. Chem.*, 1959, **24**, 1847–1854; (b) R. Luque, J. H. Clark, K. Yoshida and P. L. Gai, *Chem. Commun.*, 2009, 5305–5307; (c) M. Toba, S. Tanaka, S. Niwa, F. Mizukami, Z. Koppáby, L. Gucci, K. Cheah and T. Tang, *Appl. Catal., A*, 1999, **189**, 243–250; (d) T. Werpy, J. G. Frye, Jr., Y. Wang and A. H. Zacher, *US Pat.*, 6670300, 2002; (e) J.-A. T. Schwartz, *US Pat.*, 5478952, 1995; (f) K. H. Kang, U. G. Hong, J. O. Jun, J. H. Song, Y. Bang, J. H. Choi, S. J. Han and I. K. Song, *J. Mol. Catal. A: Chem.*, 2014, **395**, 234–242; (g) B. Tapin, F. Epron, C. Especel, B. K. Ly, C. Pinel and M. Besson, *Catal. Today*, 2014, **235**, 127–133; (h) B. K. Ly, D. P. Minh, C. Pinel, M. Besson, B. Tapin, F. Epron and C. Especel, *Top. Catal.*, 2012, **55**, 466–473; (i) B. K. Ly, B. Tapin, M. Aouine, P. Delichere, F. Epron, C. Pinel, C. Especel and M. Besson, *ChemCatChem*, 2015, **7**, 2161–2178; (j) V. N. M. Rao, *US Pat.*, 4782167, 1988; (k) K. H. Kang, U. G. Hong, Y. Bang, J. H. Choi, J. K. Kim, J. K. Lee, S. J. Han and I. K. Song, *Appl. Catal., A*, 2015, **490**, 153–162; (l) M. Konishi, K. Yokota and E. Ueno, *US Pat.*, 6706932, 2004; (m) M. Bianchi, G. Menchi, F. Francalanci, F. Piacenti, U. Matteoli, P. Frediani and C. Botteghi, *J. Org. Chem.*, 1980, **188**, 109–119.
- (a) S. Varadarajan and D. J. Miller, *Biotechnol. Prog.*, 1999, **15**, 845–854; (b) U. Stabel, H.-J. Gosch, R. Fischer, W. Harder and C. Hechler, *US Pat.*, 5073650, 1991; (c) S. Suzuki, H. Inagaki and H. Ueno, *US Pat.*, 5037996, 1991; (d) K. Turner, M. Sharif, C. Rathmell, J. W. Kippax, J. Scarlett, A. J. Reason and N. Harris, *US Pat.*, 4751334, 1988.
- (a) T. Haas, B. Jaeger, R. Weber, S. F. Mitchell and C. F. King, *Appl. Catal., A*, 2005, **280**, 83–88; (b) M. Shlaf, *Dalton Trans.*, 2006, 4645–4653.
- M. Costantini, E. Fache and D. Nivert, *US Pat.*, 5756837, 1998; A. W. John and S. L. Singrey, *US Pat.*, 3365490 A, 1968.
- M. A. Mabry, W. W. Prichard and S. B. Ziemecki, *US Pat.*, 4550185, 1985; M. A. Mabry, W. W. Prichard and S. B. Ziemecki, *US Pat.*, 4609636, 1986; B. W. Griffiths and J. B. Michel, *US Pat.*, 4659686, 1987; R. E. Bockrath, D. Campos,

- J.-A. T. Schwartz and R. T. Stimek, *US Pat.*, 6008384, 1999; J. R. Budge, T. G. Attig and S. E. Pedersen, *US Pat.*, 5473086, 1995; S. E. Pedersen, J. G. Frye Jr., T. G. Attig and J. R. Budge, *US Pat.*, 5698749, 1997; J. R. Budge, T. G. Attig and R. A. Dubbert, *US Pat.*, 5969164, 1999; J. R. Budge, T. G. Attig and R. A. Dubbert, *US Pat.*, 6486367, 2002.
- 11 Y. Takeda, M. Tamura, Y. Nakagawa, K. Okumura and K. Tomishige, *ACS Catal.*, 2015, 5, 7034–7047.
- 12 Y. Takeda, Y. Nakagawa and K. Tomishige, *Catal. Sci. Technol.*, 2012, 2, 2221–2223.
- 13 H. G. Manyar, C. Paun, R. Pilus, D. W. Rooney, J. M. Thompson and C. Hardacre, *Chem. Commun.*, 2010, 46, 6279–6281.
- 14 Z. Hu, H. Nakamura, K. Kunimori, H. Asano and T. Uchijima, *J. Catal.*, 1988, 112, 478–488.
- 15 (a) K. Lasch, L. Jörissen and J. Garche, *J. Power Sources*, 1999, 84, 225–230; (b) A. Lopez-Rubio, B. M. Flanagan, E. P. Gilbert and M. J. Gidley, *Biopolymers*, 2008, 89, 761–768.
- 16 T. Takanashi, M. Tamura, Y. Nakagawa and K. Tomishige, *RSC Adv.*, 2014, 4, 28664–28672.
- 17 J. F. Moulder, W. F. Stickle, P. E. Sobol and K. D. Bomben, *Handbook of X-ray Photo-electron Spectroscopy*, Physical Electronics Inc., Minnesota, 1995, pp. 118–119 and 174–175.
- 18 (a) Y. Amada, Y. Shinmi, S. Koso, T. Kubota, Y. Nakagawa and K. Tomishige, *Appl. Catal., B*, 2011, 105, 117–127; (b) Y. Shinmi, S. Koso, T. Kubota, Y. Nakagawa and K. Tomishige, *Appl. Catal., B*, 2010, 94, 318–326; (c) Y. Amada, S. Koso, Y. Nakagawa and K. Tomishige, *ChemSusChem*, 2010, 3, 728–736; (d) M. Chia, Y. J. Pagán-Torres, D. Hibbits, Q. Tan, H. N. Pham, A. K. Datye, M. Neurock, R. J. Davis and J. A. Dumesic, *J. Am. Chem. Soc.*, 2011, 133, 12675–12689; (e) S. Koso, H. Watanabe, K. Okumura, Y. Nakagawa and K. Tomishige, *Appl. Catal., B*, 2012, 111–112, 27–37; (f) Y. Nakagawa, Y. Shinmi, S. Koso and K. Tomishige, *J. Catal.*, 2010, 272, 191–194; (g) S. Koso, Y. Nakagawa and K. Tomishige, *J. Catal.*, 2011, 280, 221–229; (h) M. Tamura, Y. Amada, S. Liu, Z. Yuan, Y. Nakagawa and K. Tomishige, *J. Mol. Catal. A: Chem.*, 2014, 388–389, 177–187; (i) O. M. Daniel, A. DeLaRiva, E. L. Kunkes, A. K. Datye, J. A. Dumesic and R. J. Davis, *ChemCatChem*, 2010, 2, 1107–1114; (j) D. D. Falcone, J. H. Hack, A. Y. Klyushin, A. Knop-Gericke, R. Schlögl and R. J. Davis, *ACS Catal.*, 2015, 5, 5679–5695; (k) L. Ma, D. He and Z. Li, *Catal. Commun.*, 2008, 9, 2489–2495; (l) Y. Nakagawa, X. Ning, Y. Amada and K. Tomishige, *Appl. Catal., A*, 2012, 433–434, 128–134; (m) Y. Nakagawa, K. Mori, K. Chen, Y. Amada, M. Tamura and K. Tomishige, *Appl. Catal., A*, 2013, 468, 418–425.
- 19 (a) K. Chen, M. Tamura, Z. Yuan, Y. Nakagawa and K. Tomishige, *ChemSusChem*, 2013, 6, 613–620; (b) S. Liu, M. Tamura, Y. Nakagawa and K. Tomishige, *ACS Sustainable Chem. Eng.*, 2014, 2, 2535–2549; (c) S. Liu, Y. Okuyama, M. Tamura, Y. Nakagawa, A. Imai and K. Tomishige, *ChemSusChem*, 2015, 8, 628–635; (d) S. Liu, Y. Okuyama, M. Tamura, Y. Nakagawa, A. Imai and K. Tomishige, *Green Chem.*, 2016, 18, 165–175; (e) S. Liu, Y. Okuyama, M. Tamura, Y. Nakagawa, A. Imai and K. Tomishige, *Catal. Today*, 2016, 269, 122–131; (f) Y. Nakagawa, S. Liu, M. Tamura and K. Tomishige, *ChemSusChem*, 2015, 8, 1114–1132.
- 20 S. Yagyu, M. Yoshitake and T. Chikyow, *Appl. Surf. Sci.*, 2008, 254, 7835–7837.
- 21 (a) K. Chen, K. Mori, H. Watanabe, Y. Nakagawa and K. Tomishige, *J. Catal.*, 2012, 243, 171–183; (b) K. Tomishige, M. Tamura and Y. Nakagawa, *Chem. Rec.*, 2014, 14, 1041–1054; (c) K. Tomishige, Y. Nakagawa and M. Tamura, *Top. Curr. Chem.*, 2014, 353, 127–162.
- 22 G. Beamson, A. J. Papworth, C. Philipps, A. M. Smith and R. Whyman, *J. Catal.*, 2011, 278, 228–238.
- 23 G. Rupprechter, K. Hayek, L. Rendón and M. José-Yacamán, *Thin Solid Films*, 1995, 260, 148–155.
- 24 A. Cimino, B. A. De Angelis, D. Gazzoli and M. Valigi, *Z. Anorg. Allg. Chem.*, 1980, 460, 86–98.
- 25 (a) T. Ebashi, Y. Ishida, Y. Nakagawa, S.-I. Ito, T. Kubota and K. Tomishige, *J. Phys. Chem. C*, 2010, 114, 6518–6526; (b) M. Ronning, T. Gjervan, R. Prestivik, D. G. Nicholson and A. Holmen, *J. Catal.*, 2001, 204, 292–304; (c) M. Tamura, Y. Amada, S. Liu, Z. Yuan, Y. Nakagawa and K. Tomishige, *J. Mol. Catal. A: Chem.*, 2014, 388–389, 177–187; (d) N. Ota, M. Tamura, Y. Nakagawa, K. Okumura and K. Tomishige, *Angew. Chem., Int. Ed.*, 2015, 54, 1897–1900.
- 26 Y. Amada, H. Watanabe, M. Tamura, Y. Nakagawa, K. Okumura and K. Tomishige, *J. Phys. Chem. C*, 2012, 116, 23503–23514.